High Field Magnetic Resonance Facility

The High Field Magnetic Resonance Facility (HFMRF) focuses a significant portion of its research on developing a fundamental, molecular-level understanding of biochemical and biological systems and their response to environmental effects. A secondary focus is materials science, including catalysis and chemical mechanisms and processes. Staff and science consultants within this facility offer expertise in the areas of structural biology, solid-state materials characterization, and magnetic resonance imaging (MRI) techniques. Research activities in the HFMRF include:

- structure determination of large molecular assemblies such as protein-DNA (normal and damaged DNA) and protein-RNA complexes that model assemblies that may form as a cellular response to chemical or radiological insults
- examination of conformational changes in membrane protein complexes involving metal clusters using pulsed electron paramagnetic resonance (EPR)
- nuclear magnetic resonance (NMR)-based structural and functional genomics; multi-nuclear detection and catalyst and materials characterization using solid-state techniques
- non-invasive biological imaging, integrated magnetic resonance and confocal microscopy, and slow-spinning NMR to study cell systems.

Instrumentation & Capabilities

NMR and EPR Spectrometers

- 900-MHz NMR
- 800-MHz NMR
- 750-MHz NMR
- 600-MHz NMR (2 systems)
- 500-MHz NMR (2 wide bore systems and 2 narrow bore systems)
- 400-MHz, wide bore NMR
- 300-MHz, wide bore NMR (2 systems)
- Horizontal bore 2-T NMR
- EPR spectrometer with ENDOR/ELDOR capability

Additional Capabilities

- Combined optical and magnetic resonance microscope
- Low-temperature probes for metallo-protein chemistry and structure
- Virtual NMR capability enabling use and collaboration with EMSL scientists for remote users via secure shell over the internet

Since the W.R. Wiley Environmental Molecular Sciences Laboratory (EMSL) opened in October 1997, the HFMRF has operated one of EMSL's highest-volume experimental user facilities in support of local and external user research programs. During 2004, the HFMRF supported 196 projects in which 232 external scientists used the NMR spectrometers.

The research interests of staff and users include some of the most exciting areas in modern molecular biology and biochemistry:

- **Structural/Functional Genomics**. Determination of three-dimensional structures of DNA, RNA, proteins, and enzymes and their intermolecular associations. Particular interests and collaborations exist relative to protein fold classification and sequence-structure-fold relationships.
- **Biomolecular Complexes**. Understanding the molecular interactions of larger complexes of biomolecules (proteins, DNA, RNA, and mimetic membranes) that are key regulators in cell signaling and growth (e.g., DNA damage recognition and repair processes).

- **Biological Imaging**. Acquisition of imaging and corresponding chemical information in biological samples, with particular interest in development of combined magnetic resonance and optical spectroscopy techniques to observe and elucidate biological processes.
- **Solid State**. Low-gamma nuclei detection, ultra-low-temperature NMR for sensitivity enhancement, and slow-magic-angle-spinning (MAS) methodologies for nondestructive research of cells, tissues, small animals, and bacterial colonies.
- **Measurement Science and Instrumentation Development**. Development and application of novel and unique NMR instrumentation techniques for biological and environmental problems.

Capabilities

Capabilities currently available in the HFMRF are briefly describe below.

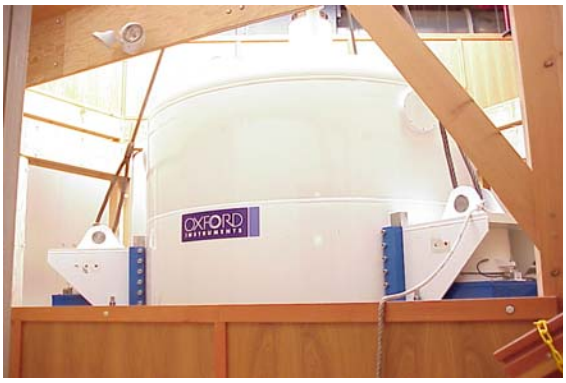

Figure 1. 900-MHz NMR magnet.

Varian INOVA 900. The Varian 900 (Figure 1) is an INOVA-based spectrometer using an Oxford 21.1-tesla (T) magnet with a 63-mm room-temperature bore. This system is capable of high-resolution liquid- and solid-state NMR. There are four radio frequency (RF) channels with waveform generators and triple-axis, pulsed-field gradients. The wideline analog digital converters (ADCs) run at 5 MHz and the narrow ADCs have a maximum rate of 500 kHz. This console also has a solids variable temperature (VT) control capability. We currently have a 5-mm HCN probe with X, Y, and Z axis gradients for liquids, a 5-mm orthogonal HX powder probe optimized for low-gamma nuclides, a 5-mm orthogonal H-N-Zn triple-tuned probe for powders, and a 3.2-mm low-gamma HX MAS probe (24 kHz spinning).

Figure 2. Varian INOVA 800.

Varian INOVA 800. The Varian 800 (Figure 2) is an INOVA-based spectrometer using an Oxford 18.8-T magnet with a 63-mm, room-temperature bore. This system is capable of high-resolution liquid- and solid-state NMR. There are four radio frequency (RF) channels with waveform generators and pulsed-field gradients. The wide-line ADCs run at 5 MHz, and the narrow-line ADCs run at a maximum rate of 500 kHz. This console also has a solids VT control capability. Available probes include two 5-mm HCN probes with Z gradient for liquids,

a 4-mm HXY MAS probe (25-kHz spinning, VT-capable), a 5-mm HX orthogonal powder probe optimized for low-gamma (38 to 65 MHz) nuclides, and a 5-mm HX static low-temperature probe (3.8 to 300 K). A 5-mm HX MAS probe (12-kHz spinning) is under construction.

Varian INOVA 750. The Varian 750 (Figure 3) is an INOVA-based spectrometer using an Oxford 17.6-T magnet with a 51-mm, room-temperature bore. This system is capable of high-resolution liquid- and solid-state NMR. There are four RF channels with waveform generators and pulsed-field gradients. The narrow ADCs have a maximum rate of 500 kHz. We currently have two 5-mm HCN probes (Z gradient), a 5-mm HCP probe (Z gradient), a 5-mm HX MAS probe (X tuning range is 321 to 130 MHz; the spinning speed is rated to 12 kHz), and two 5-mm HX MAS probes (15-kHz spinning) with X tuning ranges of 60 to 120 MHz and 30 to 50 MHz.

Figure 3. Varian INOVA 750.

Varian INOVA 600. The Varian 600 (Figure 4) is an INOVA-based spectrometer using an Oxford 14.1-T magnet with a 51-mm, room-temperature bore. This system is capable of high-resolution, liquid-state NMR. There are four RF channels with waveform generators and pulsed-field gradients. The narrow-line ADCs run at a maximum rate of 500 kHz. We currently have a 5-mm HCN probe with Z gradient and a 5-mm HX probe (X tuning range is 242 to 60 MHz). Our first 5-mm HCN cryogenic probe was installed on this system in February of 2004.

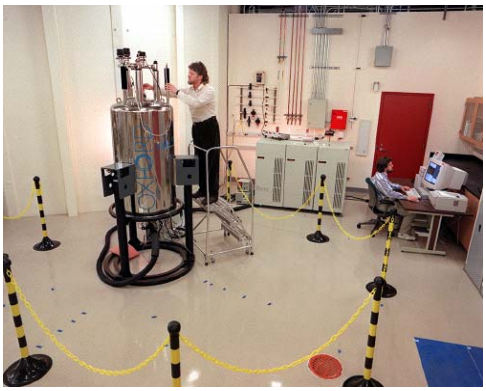

Figure 4. Varian INOVA 600.

Varian Unity 600. The Varian 600 (Figure 5) is an INOVA-based spectrometer using an Oxford 14.1-T magnet with a 51-mm, room-temperature bore. This system is capable of high-resolution, liquid-state NMR. There are three RF channels with waveform generators and pulsed-field gradients. The narrow-line ADCs run at a maximum rate of 500 kHz. We currently have a 5-mm HCN probe with Z gradient and a 5-mm HX probe (X tuning range is 242 to 60 MHz). Installation of a 5-mm pentaprobe is in progress.

Figure 5. Varian Unity 600.

Varian Unity+ 500 Wide Bore. The Varian 500 Wide Bore (Figure 6) is a Unity+-based spectrometer using an Oxford 11.7-T magnet with an 89-mm room-temperature bore. This system is capable of solid-state NMR, micro-imaging, and small-animal MRI. There are three RF channels with waveform generators. The wide-line ADCs run at 5 MHz. We currently have a 7-mm HX MAS probe (10-kHz spinning), an HX single-crystal probe, a ^{1}H CRAMPS probe, a micro-coil imaging probe, a 40-mm imaging probe, and a static HX low-temperature probe (2 to 300 K).

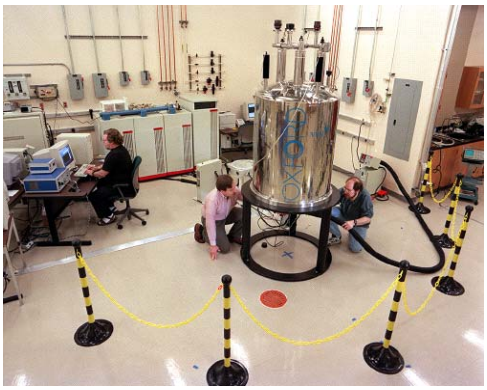

Figure 6. Varian Unity+ 500 wide bore.

Bruker Avance 500 Wide Bore. The Bruker Avance 500 Wide Bore (Figure 7) is a micro-imaging system using an 89-mm vertical room-temperature bore. The system is capable of imaging mice and also has high-resolution liquid magnetic resonance capabilities with a Bruker 10-mm QNP probe. This liquid probe has a ^{1}H outer coil and an inner coil that is switchable among ^{13}C, ^{31}P, and ^{19}F with no gradients. The system is equipped with a combined confocal and magnetic resonance microscope capable of monitoring single layers of eukaryotic cells in a perfusion system simultaneously with both modalities.

Figure 7. Bruker Avance 500 wide bore.

Varian/Chemagnetics Infinity 500. The Chemagnetics 500 (Figure 8) is an Infinity-based spectrometer using an Oxford 11.7-T magnet with a 51-mm, room-temperature bore. This system is capable of high-resolution liquid- and solid-state NMR. It has three RF channels and is equipped with both 16- and 14-bit ADCs. The solution-state probes for this instrument include a 5-mm HCN gradient probe, a 5-mm DB gradient probe (X tuning range is 208.1 to 49.5 MHz), and a 10-mm HX probe (X tuning range is 218.6 to 21.2 MHz). There are two solid-state probes, a 5-mm HX MAS probe (X tuning range is 206.6 to 47 MHz; the spinning speed is rated to 12 kHz) and a

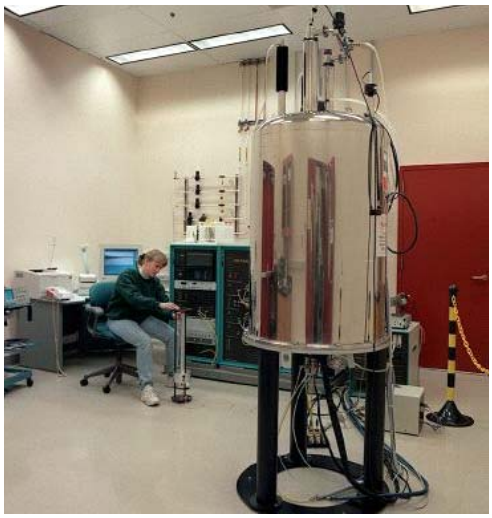

Figure 8. Varian/Chemagnetics Infinity 500.

6-mm HX MAS probe (X tuning range is 218.6 to 48.7 MHz, H/F tuning range is 510.6 to 459 MHz; the spinning speed is rated to 9 kHz).

Varian Unity+ 500 Narrow Bore. The Varian 500 (Figure 9) is a Unity+-based spectrometer using an Oxford 11.7-T magnet with a 51-mm, room-temperature bore. This system is capable of high-resolution, liquid-state NMR. There are three RF channels with waveform generators and pulsed-field gradients. We currently have a 5-mm HCN probe with Z gradients and a 10-mm HX probe.

Figure 9. Varian Unity+ 500 narrow bore.

Varian/Chemagnetics Infinity+ 400. The Varian 400 spectrometer (Figure 10) is an Infinity+-based spectrometer using an Oxford 9.4-T magnet with an 89-mm, room-temperature bore. This system is only used for solid-state NMR. There are two RF channels and a 5-MHz ADC. We currently have a 5-mm HX MAS probe, a 5-mm HX static cryogenic probe (3.8 to 300 K), a 7-mm HX static low-temperature probe (4.2 to 400 K), and a 10-mm HX DAS probe. All of the Unity+ 500 wide-bore broadband probes may be used in single-channel mode.

Figure 10. Varian/Chemagnetics Infinity+ 400.

Varian/Chemagnetics Infinity 300. The Chemagnetics 300 (Figure 11) is an Infinity-based spectrometer using an Oxford 7.02-T magnet with an 89-mm, room-temperature bore. This system is capable of high-resolution liquid- and solid-state NMR. It has three RF channels and is equipped with both 16- and 14-bit ADCs. The solution-state probes for this instrument include a 5-mm HX probe and a 10-mm HX probe. The solids probes are a 7.5-mm HX MAS probe (X tuning range is 136.7 MHz to 29.5 MHz; H tuning range is 274.7 to 349.1 MHz; spin rate is rated to 7 kHz) and a 5-mm HXY MAS probe (X tuning range is 129 to 57.4 MHz; Y tuning range is 85.1 to 21.2 MHz; spin speed is rated to 12 kHz).

Figure 11. Varian/Chemagnetics Infinity 300.

Varian Unity+ 300. The Varian 300 (Figure 12) is a Unity-based spectrometer using an Oxford 7.04-T magnet with an 89-mm, room-temperature bore. This system is capable of solid-state NMR, micro-imaging, and small-animal MRI. There are two RF channels with wide-line ADCs running at 5 MHz. We currently have a 7-mm HX MAS probe (10-kHz spinning); an HX single-crystal probe; a ^{1}H CRAMPS probe, a single-tuned HX 5-mm, low-temperature MAS probe (35 to 300K, 12-kHz spinning); a 7-mm HX high-temperature probe (-100 to 500°C, 7-kHz spinning); a microscopy probe; and a 40-mm imaging probe.

Figure 12. Varian Unity+ 300.

Horizontal Bore 2-T Magnet. The 2-T magnet (Figure 13) provides unique capabilities for the HFMRF. It is connected to a Varian Unity+ console with two RF channels and wideline 5-MHz ADC's. It has a 30-cm room-temperature bore and is equipped with an imaging gradient set capable of 50 gauss/cm. It is suitable for small animal or large sample imaging and *in vivo* spectroscopy. Three homemade birdcage coil probes are available: 8-cm and 5-cm imaging/spectroscopy probes and a 5-cm ^{3}He probe.

Figure 13. Horizontal bore 2-T magnet.

Bruker Pulsed EPR/ENDOR/ELDOR Spectrometer. This multi-functional pulsed EPR spectrometer (Figure 14), operating in the X-band near 9.5 GHz, permits application of modern pulsed magnetic resonance techniques to systems containing unpaired electron spins. The system is based on the Bruker EleXsys console and SuperX-FT microwave bridge, which allow both ELDOR (electron-electron double resonance) and ENDOR (electron nuclear double resonance) measurements. A number of probes for both continuous-wave and pulsed spectroscopy are included, with an operating temperature ranging from room temperature to below liquid helium. System capabilities include measurement of g-tensors; hyperfine and nuclear quadrupole-coupling tensors for the study of electronic wavefunction of free radicals and metalloproteins; and determination of small dipolar interactions by pulsed ELDOR and double electron-electron resonance methods for the measurement of distances between radicals in solids or between spin labels in proteins.

Figure 14. Bruker pulsed EPR/ ENDOR/ ELDOR spectrometer.

Upgrades

600-MHz Cold Probe. In early 2004, the HFMRF enhanced available NMR capabilities with the arrival of an H(C/N) pulsed-field-gradient, triple-resonance cold probe (Figure 15) for the 600/51 Inova NMR system. The probe was delivered on January 23, 2004, and installation was complete by February 23. The cold probe system has been available to users since March 3, and has contributed to the collection of high-quality data for a number of peer-reviewed scientific projects. The benefits of the cold probe system to EMSL users include a reduction in system thermal noise and a three- to fourfold increase in signal-to-noise performance. Greatly improved signal-to-noise performance allows the user either to reduce data collection times, increasing the number of experiments that can be performed in a given time slot, or to reduce sample concentrations to examine more challenging sample systems. The improvement in productivity afforded by the cold probe, as well as the ability to examine less tractable systems by NMR, increase the HFMRF's ability to support leading-edge scientific research.

Figure 15. 600-MHz cold probe.

600-MHz INOVA Console and Pentaprobe. The 600-MHz INOVA console (Figure 16) upgrade replaced a 14-year-old Unity console that had been used on the system since it was delivered. The original console, superseded by two generations of console architecture, could not run the current generation of software. Our new console is capable of running the state-of-the art suite of biological experiments, BioPack, that simplifies the collection of protein structure data. BioPack has an automated calibration module that makes experiment setup more efficient and offers a range of experiments that could not be performed on the old console. The new console also features a deuterium-decoupling channel that opens up a new range of samples and experimental approaches to collecting protein structure data on large proteins. As part of the console upgrade, a HNCPD probe was purchased, which will increase signal-to-noise performance on the existing experiments as well as adding capability for additional structural experiments on RNA and DNA. This probe is being installed for use in early 2005.

Figure 16. 600-MHz INOVA console and pentaprobe.

900-MHz NMR Magnet. The 900-MHz NMR (Figure 17) had all installation and acceptance tests completed in late 2003. The system's first user three-dimensional spectrum was completed in early December 2003 on a three-protein complex (BRCA1/BARD1/UbCh5c), a biomolecular system important in the study of breast and ovarian cancer development. The 900-MHz NMR has been in regular scheduled use since January 2004. We had 24 users on the system through the end of September 2004. The data quality for both liquid- and solid-state experiments has been outstanding, especially for the "through space" nuclear Overhauser effect experiments. Taking advantage of the system's 63-mm bore (wider than the industry standard), we have been optimizing experiments and building probes for solid-state capability. At present, three probes are available for solid-state experiments (described below) for samples in environmental, bioinorganic, catalysis, and materials studies, and two probes are available for high-resolution liquid NMR experiments that are primarily intended for structure determination and dynamics studies of biomolecular complexes and large macromolecules. Overall, the 900-MHz NMR system has been performing very well. Throughout 2004, we have been gaining experimental and operational experience yielding superior results to our other high-field systems.

Figure 17. 900-MHz NMR magnet.

Solid-State NMR Probe Development. Researchers from the HFMRF and Pacific Northwest National Laboratory are developing unique solid-state probes. One of these unique probes, a cryogenic solid-state NMR probe, is shown in Figure 18 along with its developers. In the last year, we have created several new probes. We built two new cryogenic probes for the 9.4-T and 11.7-T magnets. The 11.7-T probe is a static triple-tuned HXY probe, and the 9.4-T probe is a static HX probe capable of tuning from ^{25}Mg to ^{31}P. The techniques used to develop new capacitor and vacuum feed required by these probes have enabled all of the tuning elements to be located in the cryogenic environment; therefore, the tuning ranges are no longer limited, and the probes can be tuned to a wide range of nuclei. Also, a new slow-spinning 5-mm CPMAS probe was built for use in the Varian and Bruker imaging gradients sets. This probe is enabling a new class of experiments to be implemented that are primarily used for studying metabolic changes in cellular systems. For the 21.1-T magnet (900-MHz NMR), a high-speed 3.2-mm CPMAS HX probe with a tuning range of strontium-87 to sodium-23 is the first CPMAS probe developed for this magnet. Because of its high spinning speed (>23 kHz) and its high-performance RF section, this probe will enable several new solid-state experiments to

Figure 18. Cryogenic solid-state NMR probe and its developers.

be run at this high field. One of the first user projects to benefit from the new probe is a study of environmentally challenging clean-up samples containing strontium.

EPR Console and Pulsed Bridge. The original console and microwave bridge on the pulsed EPR/ENDOR/ELDOR spectrometer were upgraded in November 2004 to an EleXsys E580 console and a SuperX-FT bridge. This upgrade provides a modern operating system and user interface for the spectrometer, and enables remote operation of the spectrometer over the Internet. A great improvement in resolution and throughput are afforded by the new pulse programmer and signal averager in the new console, and with many samples, a tenfold increase in signal-to-noise performance is achievable. The microwave bridge offers improved sensitivity and pulse-shaping ability, and is capable of producing microwave pulses as narrow as 2 ns. Two independent microwave sources in the bridge permit routine pulsed ELDOR measurements of nanoscale distances and facilitate a number of hyperfine selective ENDOR measurements. The SuperX-FT bridge includes a strip-line, pulse-former unit with four microwave channels, and a pair of microwave pulse former units that provide four additional microwave channels in addition to the ELDOR channel. Pulse sequences are being ported over to the new system, and calibrated data collection for research projects is currently underway. The new console is supported by a new Xepr data analysis software suite and the Xsophe simulation suite, with enhanced, extensible processing and simulation of experimental data.

Future Directions

As the HFMRF prepares to meet the requirements of the two new EMSL Grand Challenges and strategically fit the facility resources to match capability needs of some of the future Collaborative Access Team (CAT) proposals, careful efforts will be needed to select resource enhancements, equipment updates, and novel capability developments. This will require adding some capabilities that will have obvious impacts to data collection of a large number of projects, Grand Challenges, CATs, and many open-call proposals. These additions could include purchase of a cold probe for a high-field instrument or investment in more specific capabilities, such as a unique probe design to help with *in situ* catalysis experiments as part of the Catalysis CAT. The needs for the Grand Challenges will be emerging in 2005 as scientific milestones are set.

Recent upgrades to the pulsed EPR spectrometer will expand the range of experiments that are possible for the Biogeochemistry Grand Challenge. Designing a new "flat-coil" probe for use with bio-solid-state experiments could help with the study of protein-membrane orientation, both in cyanobacterium and other systems identified by our user base. This type of probe, paired with our 900-MHz NMR, could yield a powerful combination for gaining new understanding of membrane biology. With a strong footing in the study of radionuclides on a 300-MHz NMR system, we have the potential to advance another unique capability here at EMSL.

In the fall of 2005, we plan to receive an 800-MHz, cold-probe system that was purchased in mid-2004. This system will have the highest signal-to-noise capability of all our biological liquid NMR probes (about a 50% increase over the 600-MHz cold-probe system received in 2004.) This will be a welcome improvement for difficult samples, such as larger

macromolecules and other samples less tractable at milli-molar concentrations. New sample systems that were previously intractable for study with the previous technology will be practical at tens of micro-molar concentrations.

Other capability-development projects that may be pursued in 2005 include a 4-mm HX CPMAS (VT-capable; strontium-87 to sodium-23) for the 900-MHz NMR spectrometer that could help with a variety of solid-state material projects and would add needed sensitivity to help with studying the strontium environmental clean-up project.

Looking for opportunities to support distinguishing science capabilities, as well as maintaining our systems as state-of-science, will keep our facility productivity high and its capabilities relevant. One of our lower-field systems, primarily used for programmatic work, was retired from the user facility on October 1, 2004. The user projects formerly supported on this system will be shifted to other facility systems. Evaluations of facility scope and resource needs are ongoing.

A Radius of Curvature Analysis of a 16-Base-Pair DNA Oligomer Provides New Insight into Global DNA Curvature

K McAteer,[(a)] A Aceves-Gaona,[(a)] R Michalczyk,[(b)] GW Buchko,[(c)] NG Isern,[(d)] LA Silks,[(b)] JH Miller,[(a)] and MA Kennedy[(c)]

(a) Washington State University Tri-Cities, Richland, Washington
(b) Los Alamos National Laboratory, Los Alamos, New Mexico
(c) Pacific Northwest National Laboratory, Richland, Washington
(d) W.R. Wiley Environmental Molecular Sciences Laboratory, Richland, Washington

Intrinsic DNA curvature plays a role in many cellular processes including transcription regulation, and is important in DNA-protein and DNA-drug interactions. The study of this relatively long 16-base-pair DNA not only provides insight into the necessity of using residual dipolar couplings in NMR-based DNA structure analysis, but also indicates that the existing general models used to explain DNA bending are insufficient.

In-phase ligated DNA containing T_nA_n segments fail to exhibit the retarded polyacrylamide gel electrophoresis (PAGE) migration observed for in-phase ligated A_nT_n segments, a behavior thought to be correlated with macroscopic DNA curvature. The lack of macroscopic curvature in ligated T_nA_n segments is thought to be caused by cancellation of bending in regions flanking the TpA steps. To address this issue, solution-state nuclear magnetic resonance (NMR) spectroscopy, including residual dipolar coupling (RDC) restraints, was used to determine a high-resolution structure of [d(CGAGGTTTAAACCTCG)2], a DNA oligomer containing a T_3A_3 tract (McAteer et al. 2004). The overall magnitude and direction of bending, including the regions flanking the central TpA step, was measured using a radius of curvature (R_c) analysis. The R_c for the overall molecule indicated a small magnitude of global bending (R_c = 138 ± 23 nm) towards the major groove, whereas the R_c for the two halves (72 ± 33 nm and 69 ± 14 nm) indicated greater localized bending into the minor groove. The direction of bending in the regions flanking the TpA step is in partial opposition (109°), contributing to cancellation of bending. The cancellation of bending did not correlate with a pattern of roll values at the TpA step, or at the 5´ and 3´ junctions, of the T_3A_3 segment, suggesting a simple junction/roll model is insufficient to predict cancellation of DNA

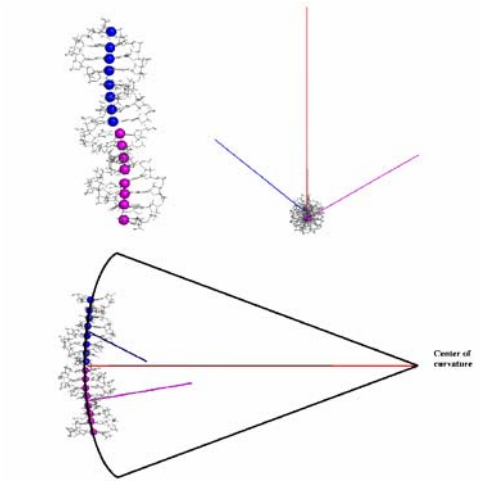

Figure 1. Global curvature of the average RDC structure (top left) of the T_3A_3 16mer analyzed by fitting a circle to the helical axis reference points (blue/pink balls). (b) R_c for the whole molecule (red), and for the upper (blue) and lower (pink) halves, looking parallel to the helix axis (top right). (c) R_c for the whole molecule (red) and for the upper (blue) and lower (pink) halves, looking perpendicular to the helix axis (bottom).

bending in all T_nA_n junction sequence contexts; more importantly, R_c analysis of structures refined without RDC restraints lacked the precision and accuracy needed to reliably measure bending.

Reference

McAteer K, A Aceves-Gaona, R Michalczyk, GW Buchko, NG Isern, LA Silks, JH Miller, and MA Kennedy. 2004. "Compensating Bends in a 16-Base-Pair DNA Oligomer Containing a T_3A_3 Segment: A NMR Study of Global DNA Curvature." *Biopolymers* 75(6):497-511.

Carbon Functional Groups of Plant Material and Soil Organic Matter Density Fractions: Land Use Effects

E Marín-Spiotta,[(a)] SD Burton,[(b)] MS Torn,[(c)] and WL Silver[(a)]

(a) University of California, Berkeley, Berkeley, California
(b) W.R. Wiley Environmental Molecular Sciences Laboratory, Richland, Washington
(c) Lawrence Berkeley National Laboratory, Berkeley, California

We used solid-state ^{13}C NMR spectroscopy to determine the degree of decomposition of soil organic matter fractions along a land-use chronosequence. This work is part of a larger study on the importance of conditions for carbon sequestration. Chemical and physical protection mechanisms influence soil carbon sequestration depending on geological and land-use conditions.

Soils store almost three times as much carbon as aboveground plant biomass and can exert a strong influence on the atmospheric concentration of carbon dioxide through their role as carbon sources or sinks. Scientific and political interest in the carbon sink potential of soils has emphasized the need to understand the controls on soil carbon turnover and the formation of stable, recalcitrant carbon pools in soils. Soil organic matter (SOM), of which about 50% by weight is composed of carbon, is a heterogeneous mixture of plant, animal, and microbial residues that represents a continuum of decay (Kögel-Knabner 1993). Recent advances in nuclear magnetic resonance (NMR) spectroscopy, such as solid-state applications, have proven to be useful tools for the study of the structural chemistry of SOM *in situ* with little or no chemical modifications.

Our research has two objectives: 1) to determine the effect of changes in the chemical composition of plant litter inputs on soil organic carbon chemistry and 2) to determine the degree of decomposition of SOM carbon fractions in different associations with the mineral soil matrix. To accomplish these objectives, we acquired solid-state, cross-polarization magic angle spinning (CPMAS) ^{13}C-NMR spectra of plant and soil samples on a Varian Infinity CMX 300-MHz NMR spectrometer at the W.R. Wiley Environmental Molecular Sciences Laboratory (EMSL). In particular, we examined the similarities and differences between spectra of whole-leaf litter samples, lignin extracts of whole-leaf litter, and two different SOM fractions. These soil carbon fractions are the results of a physical density separation procedure that separated the SOM into a free particulate organic matter fraction and an occluded organic matter fraction, released after the disruption of soil aggregates. This research is part of a larger study led by W.L. Silver at the University of California, Berkeley, on the importance of chemical and physical protection mechanisms on soil carbon sequestration during a land-use chronosequence of secondary forests regrowing on abandoned pastures.

^{13}C-NMR spectroscopy provides information on the relative abundance of organic carbon functional groups such as alkyl carbon (0 to 45 ppm), O-alkyl carbon (50 to 110 ppm), aromatic carbon (110 to 160 ppm), and carbonyl carbon (160 to 220 ppm), which can be used as indicators for the presence of different compound groups. Recent applications of ^{13}C-NMR to SOM studies have shown a decrease in the intensity of the O-alkyl carbon area and an increase in the alkyl and aromatic carbon region from the free light fraction to the occluded light fraction, suggesting an increase in structural modification and, thus,

decomposition from one fraction to the other (Baldock et al. 1992). Alkyl-carbon structures in SOM have been hypothesized to represent hydrophobic (non-polar) compounds categorized as soil lipids, which are thought to be highly resistant to decay (Kögel-Knabner et al. 1992). It is not known what proportion of soil lipids is directly derived from plants (waxes, cutin, suberin, and terpenoids), and how much is microbially derived or produced *in situ* during humification.

In our study, we found that fresh leaf plant material from active pastures differed from that of forests in the intensity of all four spectral regions examined, suggesting the two ecosystem types have remarkably different structural carbon chemistries. Forests had greater proportions of their spectra contributed by alkyl, aromatic, and carbonyl carbon functional groups than pastures, which had greater contributions by O-alkyl carbon. The extraction procedure for Klason lignin (Ryan et al. 1990) resulted in the loss of intensity of the carbohydrate signal at 72 ppm, attributed to cellulose in whole plant leaf material, and a gain in signal intensities at 28 ppm, representative of long-chain aliphatics, and in the aromatic region (Figure 1). The NMR spectra of the two soil carbon fractions differed from that of the starting leaf plant material in all regions except for the alkyl region, which may suggest the conservation of aliphatic material derived from leaf cuticle waxes. Interestingly, the striking differences between forest and pasture starting leaf material are lost as the material gets incorporated into the SOM pool, and there are no obvious land-use vegetation differences in the soil carbon fractions.

Analysis of the four different spectral regions did not result in statistically significant differences between the free particulate and occluded SOM fractions. Visual differences in the spectra, however, suggest a greater intensity of carbon in the alkyl and aromatic regions in the occluded fraction as carbon gets incorporated into soil aggregates (Figure 1). The ratio of alkyl to O-alkyl

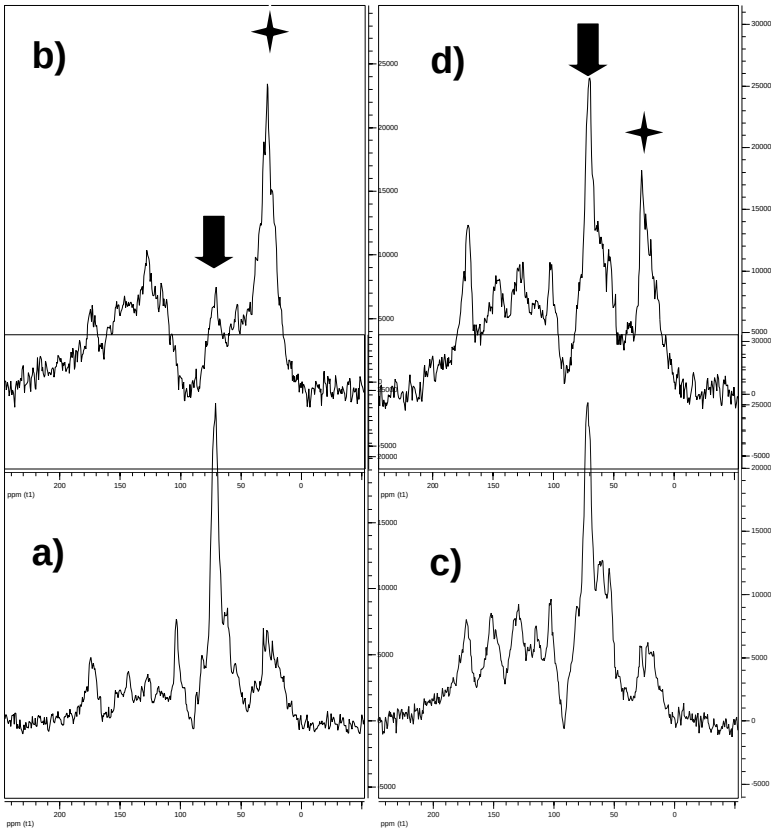

Figure 1. ^{13}C-NMR spectra of a) whole-leaf litter, b) Klason lignin extract from leaf litter, c) free, particulate SOM density fraction, and d) occluded SOM density fraction from a forest site. The arrows indicate peaks at 73 ppm and the stars indicate peaks at 28 ppm.

regions, which has been proposed as a measure of the degree of oxidation or decomposition of SOM (Baldock and Preston, 1995), is marginally higher in the occluded fraction than the free particulate SOM fraction.

We will combine the results on carbon functional groups in the soil density fractions derived from our ^{13}C-NMR analyses with residence time estimates as determined from stable and radiocarbon isotope techniques to determine whether differences in carbon chemistry and organic matter location outside or within soil aggregates translate into differences in turnover rates. This information will help us better understand the physical and chemical mechanisms that control SOM stability in soils. A better understanding of the controls on soil carbon storage will improve our ability to model belowground dynamics and thus enhance our capacity to rehabilitate degraded soils, assess the potential for carbon sequestration in soils, and increase our ability to predict the effects of future human disturbance or climatic change on soil carbon pools.

References

Baldock JA, JM Oades, AG Waters, X Peng, AM Vasallo, and MA Wilson. 1992. "Aspects of the Chemical Structure of Soil Organic Materials as Revealed by Solid-State ^{13}C-NMR Spectroscopy." *Biogeochemistry* 16(1):1-42.

Baldock JA and CM Preston. 1995. "Chemistry of Carbon Decomposition Processes in Forests as Revealed by Solid-state Carbon-13 Nuclear Magnetic Resonance." In *Carbon Forms and Functions in Forest Foils,* eds. WW McFee and JM Kelly, pp. 89-117, Soil Science Society of America, Inc., Madison, Wisconsin.

Kögel-Knabner I, JW de Leeuw, and PG Hatcher. 1992. "Nature and Distribution of Alkyl Carbon in Forest Soil Profiles: Implications for the Origin and Humification of Aliphatic Biomacromolecules." *The Science of the Total Environment* 117(118):175-185.

Kögel-Knabner I. 1993. "Biodegradation and Humification Processes in Forest Soils." *Soil Biochemistry*, ed. JM Bollag and G. Stotzky, Dekker, New York.

Ryan MG, JM Melillo, and A Ricca. 1990. "A Comparison of Methods for Determining Proximate Carbon Fractions of Forest Litter." *Canadian Journal of Forest Research* 20(2):166-171.

Hydrogen Storage Materials

WJ Shaw,[(a)] JC Linehan,[(a)] and ST Autrey[(a)]
(a) Pacific Northwest National Laboratory, Richland, Washington

Hydrogen offers a potential clean energy source; however, new solid materials with high volume storage capacities are needed. A fundamental understanding of these materials is necessary for further development.

The increasing demands for clean energy sources that do not add more carbon dioxide and other pollutants to the environment have resulted in increased attention worldwide to the possibilities of a 'hydrogen economy' as a long-term solution for a secure energy future based on potentially renewable resources. Some of the greatest challenges are the discovery and development of new on-board hydrogen storage materials and catalysts for vehicles powered by fuel cells. New materials that store both high-gravimetric, high-volumetric densities of hydrogen that release hydrogen at temperatures below 100ºC and uptake hydrogen at pressures lower than 100 bar are highly desired. The volumetric constraints eliminate pressurized hydrogen systems from consideration and lead development efforts toward the development of solid storage materials. There are no currently known materials that meet these requirements. As such, there is a need for fundamental understanding of the chemical and physical properties of hydrogen-rich materials (HRM). What molecular attributes facilitate the release and uptake of molecular hydrogen?

We suggest that efficient storage of hydrogen might be accomplished in compounds that have alternating electron-rich and electron-deficient sites capable of covalently binding H^+ and H^-, respectively. There are two fundamental premises that will guide us toward the discovery of novel HRMs that are operational at temperatures between ambient and 100°C: 1) binding of hydrogen requires formation of chemical bonds, as physisorption of hydrogen is too weak, and 2) inherent polarity of low molecular weight species bearing electron-rich and electron-deficient sites will likely result in the formation of molecular solids.

These guidelines led us to initially consider ammonia borane (AB = NH_3BH_3). AB is isoelectronic with ethane. This inorganic analog of ethane yields far more favorable volumetric densities, as it is a solid (melting point 115°C) rather than a gas. This molecular crystal is formed from the reaction of ammonia with diborane to form a dative bond between the electron-deficient boron and the electron-rich nitrogen ($NH_3 \rightarrow BH_3$). The molecular crystalline solid is further composed of a network of dihydrogen bonds formed between the protic H^+ attached to nitrogen and the hydridic H^- attached to boron.

Preliminary experimental results showed the rates of hydrogen release from the bulk phase solid AB follows an apparent nucleation and growth kinetic model. However, little is known about the nucleation events and the role of the intermolecular dihydrogen bonding in the formation of molecular hydrogen. Solid-state nuclear magnetic resonance (ssNMR) $^{11}B\{^1H\}$ spectra of these reactions taken at 300 MHz ^1H frequency aided in determining reaction mechanisms; however, some products remain unidentified because of spectral overlap. NMR experiments run at higher fields enhanced the resolution and reduced the quadrupolar coupling to identify all reaction products as a result of hydrogen release and simplified the distinction between quadrupolar coupling and multiple species (Figures 1

and 2). In some cases, a 500-MHz field was adequate, but in other cases, an 800-MHz field was needed to identify some of the products, as shown in Figure 2.

In addition to ^{11}B ssNMR, ^{1}H ssNMR spectra were also taken at 800 MHz. Each of the starting materials and reaction products were studied. As expected, chemical shift differences were observed. These observations will be further quantified using heteronuclear chemical shift correlation to correlate the ^{1}H and ^{11}B resonances to provide further product identification.

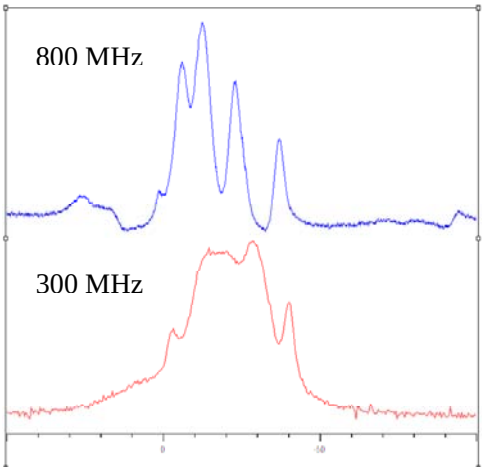

Figure 1. $^{11}B\{^{1}H\}$ ssNMR (spinning speed 10 kHz) of NH_3BH_3 reaction products as a function of field. The increased resolution at 800 MHz allowed identification of two new products.

One particularly interesting observation from ^{1}H spectra is shown in Figure 3. In addition to investigating the NH_3BH_3 as a function of applied heat, we have also found that scaffolding the NH_3BH_3 into mesoporous silica reduces the temperature for hydrogen release. The chemistry and thermodynamics behind this observation are not understood; however, the extreme narrowing in the proton NMR spectrum would suggest either an increased ordering or a more liquid-like behavior in the scaffold. Further experiments such as rotational-echo double-resonance are necessary to propose a mechanism, but the initial insight provides evidence of a fundamentally different organization within the scaffold.

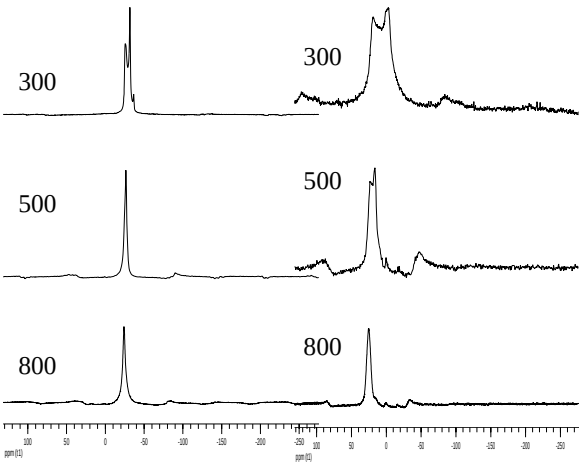

Figure 2. ssNMR $^{11}B\{^{1}H\}$ spectra as a function of field, spinning at 10 kHz. The starting material (left) and the final reaction products (after heating at 170°C [right]) are shown at all three fields. For some compounds, such as NH_3BH_3 (left), 500 MHz provides maximum narrowing. For some of the products (right), 800 MHz is needed to sufficiently narrow the peaks. Investigating at all three fields provides important information about the coupling constant, the symmetry, and the products.

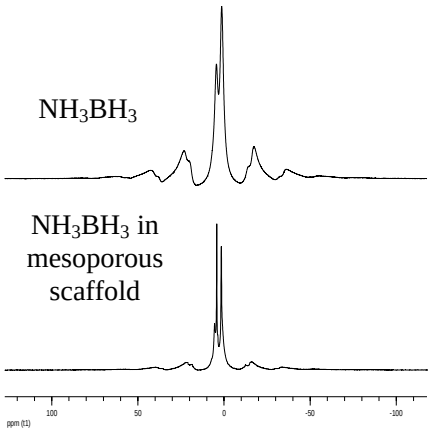

Figure 3. ^{1}H ssNMR (spinning speed 15 kHz) reveals a distinct narrowing of the two resonances as a function of scaffolding NH_3BH_3 into mesoporous silica.

Investigating Molecular Recognition and Biological Function at Interfaces Using Antimicrobial Peptides

SM Jones,[(a)] YN Nikolayeva,[(a)] JJ Ford,[(b)] DW Hoyt,[(b)] and M Cotten[(a)]
(a) Pacific Lutheran University, Tacoma, Washington
(b) W.R. Wiley Environmental Molecular Sciences Laboratory, Richland, Washington

By studying the mechanism of action of antimicrobial peptides from fish, we hope to better understand molecular recognition and biological function at interfaces. Such studies may also translate into knowledge needed to fight many diseases and design new drugs, including broad-spectrum drugs, by providing a more fundamental understanding of the mechanisms involved.

This research project initiated in 2003 investigates the principles underlying molecular recognition and biological function at interfaces. The focus has been on membrane-interacting, amphipathic, cationic, antimicrobial peptides (ACAPs). Natural ACAPs are water-soluble, cationic, partly hydrophobic, relatively short peptides (6 to 50 residues) that can have broad-spectrum antibacterial, fungicidal, hemolytic, virucidal, and tumoricidal activities. Their initial targets appear to be negatively charged microbial membranes. Their amphipathic structures, molecular volumes, and aggregation states in solution and the lipid membrane have been considered important for their function and mechanism of action. Therefore, characterizing their three-dimensional structures in the membrane-bound state plays a determinant role in the search for relationships between their structural motifs, interactions with biological membranes, potency, and mechanisms of action. These studies can be challenging, however, the use of membrane-mimetic systems has allowed tremendous progress in determining the impact of specific parameters on their function and structure. In fact, it is now realized that fully understanding how ACAPs work may involve studying the possible synergy between several functions at the membrane and intracellular levels. Overall, it is clear that much information remains to be learned about the initial interactions of ACAPs with membranes and the events unfolding thereafter.

The ACAPs investigated in this research are piscidins, which were discovered in fish immune mast cells (gills, skin, and guts) (Silphaduang 2001). They are not only the first ACAPs ever found in the mast cells of animals, but they are also believed to play a crucial, direct role in the fight against many infections. Three piscidins (piscidins 1, 2, and 3), each 22 amino acids long, have been isolated. Peculiar features of piscidins include 1) an amidated form, apparently not hemolytic for human red blood cells; 2) tolerance to high salt concentrations; 3) highly conserved amino ends; 4) highly cationic charges; and 5) high content of histidine, an aromatic amino acid.

Performing traditional structural/dynamic methods on physiologically relevant samples of membrane-bound peptides is challenging and/or not site-specific. Solid-state nuclear magnetic resonance (ssNMR) offers major advantages for probing local structure and dynamics and the precise nature of peptide-lipid interactions under changing conditions (e.g., temperature, hydration, and pH). In this project, our strategy has been to structurally characterize peptide-lipid samples using complementary ssNMR techniques. This report includes structural results for piscidin 1, the most active of the three piscidins.

Our circular dichroism (CD) studies, performed on the AVIV 62DS CD spectrometer at the W.R. Wiley Environmental Molecular Sciences Laboratory, have confirmed earlier findings that the peptide is random coil in a phosphate buffer, but it is α-helical when 50% TFE (2,2,2,-trifluoroethanol) is present in solution. Very interestingly, we have discovered that the peptide exhibits the profile typical of an α-helical structure when it is added to suspensions of large unilamellar vesicles 20% anionic phosphoglycerate, phosphatidylglycerol (PG)/80% neutral phosphocholine, phosphatidylcholine (PC), 1:30 and 1:150 peptide to lipid ratio, pH 6.2 and 7).

Using samples containing $^{13}C_i/^{15}N_{i+4}$-labeled piscidin 1, the peptide secondary structure has been investigated. Last year, we reported that the observed ^{13}C carbonyl chemical shifts in the presence of lipids were consistent with an α-helical structure. We have now made significant progress in measuring $^{13}C_i/^{15}N_{i+4}$ distances along the peptide backbone using rotational-echo double-resonance (REDOR) (Guillion and Shaefer 1989) to determine if hydrogen bonds characteristic of α-helical secondary folds are present in piscidin 1 in the presence of hydrated lipid bilayers. If the peptide is α-helical, we expect the $^{13}C_i/^{15}N_{i+4}$ distance to be about 4.1 to 4.2 Å. If the peptide structure is random coil or β-sheet, the distance will be too long to be detected. We have performed ^{13}C-detect REDOR so the use of ether-linked PC and PG lipids has avoided overcrowding in the carbonyl region, and only peptide signal is now detected in that area. These lipids have proven to be reliable substitutes for the ester-linked lipids (Lam et al. 2001). As a starting point for this study, saturated C14 PC and PG lipids mixed in molar ratio of 3:1 have been used to mimic microbial membranes.

Our present setup for the distance measurements includes a low temperature setting (approximately -50°C) to quench some dynamics problematic at room temperature in the hydrated peptide/lipid samples of interest. The samples were hosted in Kel-F cells machined at the W.R. Wiley Environmental Molecular Science Laboratory (EMSL). Figure 1 shows our updated REDOR data suggesting that within experimental errors, the $^{13}C_1$-Ile$_{16}/^{15}$N-V$_{20}$ (I$_{16}$V$_{20}$) distance is consistent with an α-helical structure. The data for the $^{13}C_1$-Gly$_8/^{15}$N-V$_{12}$ (pH 7.35) is in agreement with this finding. This is also consistent with our preliminary CD studies done under similar sample conditions.

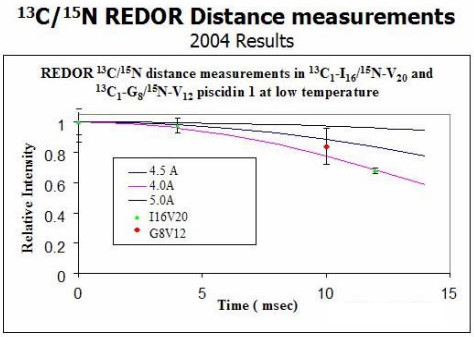

Figure 1. $^{13}C/^{15}N$ REDOR distance measurements performed on piscidin 1 bound to hydrated lipid bilayers (1:20 peptide to lipid ratio, 80% PC/20% PG).

Future work includes the study of the $^{13}C_1$-Ile$_{16}/^{15}$N-V$_{20}$ distance. We will also initiate some complementary work on oriented samples thanks to EMSL's access to two new flat coil probes. Orientational restraints will be important to further characterize the structure at high resolution and to determine the orientation of the peptide with respect to the bilayer normal.

Piscidins are particularly interesting because they kill a broad range of fish pathogens without reported resistance and their chemical features are quite unique. Because their function is not yet known, the results of the research proposed here could be very significant. From a general standpoint, more knowledge about molecular recognition at interfaces will be gained, which could help improve the selection and design of peptides with increased antimicrobial activity and reduced toxicity.

References

Gullion T and J Schaefer. 1989. "Detection of Weak Heteronuclear Dipolar Coupling by Rotational-Echo Double-Resonance NMR." *Advances in Magnetic Resonance*, ed. WS Warren, Academic Press, San Diego, California.

Lam YH, SR Wassall, CJ Morton, R Smith, and F Separovic. 2001. "Solid-State NMR Structure Determination of Melittin in a Lipid Environment." *Biophysical Journal* 81(5):2752-2761.

Silphaduang U and EJ Noga. 2001. "Antimicrobials: Peptide Antibiotics in Mast Cells of Fish." *Nature* 414(6861):268-269.

Microscopic View of Strontium Interactions in Crystalline Solids and Environmental Materials

GM Bowers[(a)] and KT Mueller[(a)]
(a) Pennsylvania State University, University Park, Pennsylvania

Characterization of strontium in clay minerals and zeolites using solid-state nuclear magnetic resonance will contribute toward an understanding of strontium/mineral interactions in soils exposed to leaking tank waste, thus enabling the design of better models for predicting the fate of strontium in the environment.

The interactions of strontium with clay minerals and zeolites are not well understood. These interactions must be researched so accurate models can be developed for predicting the environmental fate of radioactive strontium-90 released from sites, such as the U.S. Department of Energy's Hanford Site in Washington. Solid-state nuclear magnetic resonance (ssNMR) is a useful tool for probing the molecular structure of materials including the interactions of cations sorbed by mineral systems. However, there is only one NMR-active isotope of strontium (strontium-87), and the direct study of strontium with ssNMR is experimentally challenging. Strontium-87 has similar chemistry to strontium-90 and has a quadrupolar nucleus (I = -9/2) with a low natural abundance (approximately 7%), a low gyromagnetic ratio (γ = -1.163 x 10^7 1/T·s), and large quadrupolar coupling constants (14 to 25 MHz) (Larsen et al. 2000; Bastow 2002). These factors contribute to a lack of sensitivity that must be overcome to perform time-efficient studies of strontium in natural samples, such as environmentally relevant clay minerals and zeolites. In an attempt to characterize the local electromagnetic environment of strontium nuclei in these systems, we are examining sensitivity-enhancing techniques using crystalline strontium samples and strontium-saturated clays and zeolites. In these ongoing studies, we are using the 21.14-T (^{1}H resonance frequency of 900 MHz) instrument at the W.R. Wiley Environmental Molecular Sciences Laboratory (EMSL) at Pacific Northwest National Laboratory.

The sensitivity of low-γ quadrupolar nuclei (such as strontium-87) can be maximized by performing experiments at the highest available external field strength. It is well known that the contribution to the width of a resonance caused by the quadrupolar interaction decreases with increasing external field strength. Additionally, the Curie law predicts that the population difference of the central transition increases with increasing field strength, a factor that can be important for insensitive nuclei such as strontium. Indeed, a comparison of strontium-87 static echo spectra collected at 11.74 T (^{1}H resonance frequency of 500 MHz) and 21.14 T demonstrate a twofold reduction in line width (Figure 1). This reduction in width accompanied a fourfold reduction in the required experimental time at 21.14 T to achieve a similar level of signal-to-noise reduction, demonstrating that the use of high field is integral to the study of strontium nuclei in a time-effective manner.

In addition to static Hahn-echo experiments, we investigated the combined advantages of the QCPMG pulse sequence and a 21.14-T field for acquiring strontium spectra. The QCPMG experiment is a variation on the Hahn echo sequence in which a traditional echo experiment is followed by a series of additional inversion pulses and subsequent full echo acquisitions. Spectra constructed from the resulting NMR signal contain a series of sharp peaks spaced in frequency by the inverse of the time between echo maxima in the NMR

signal. These sharp peaks map the static powder pattern, resulting in improved sensitivity while preserving the information contained in the shape of the powder pattern. QCPMG experiments were applied to strontium carbonate, nitrate, and sulfate. In these salts, improvements in sensitivity over spectra obtained using a static echo experiment at 21.14 T were observed. For the strontium sulfate resonance, it was possible to acquire a spectrum with clearly visible features in 4 hours with the QCPMG sequence and a 1-kHz spikelet spacing vs. 24 hours with an echo at 21.14 T. Iterative simulations of the resulting spectra are currently in progress to determine the quadrupolar and chemical shift parameters for each salt sample.

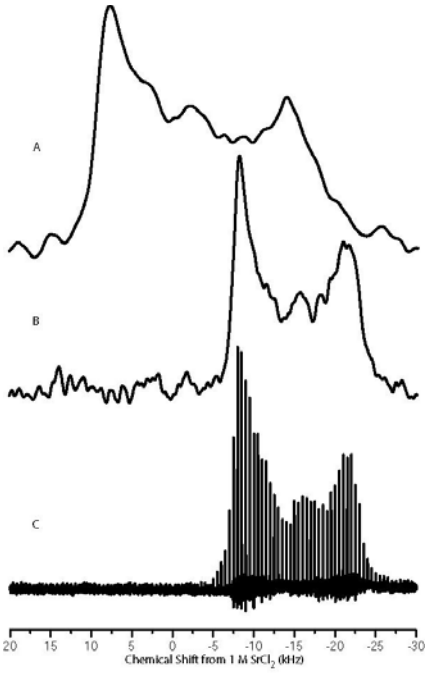

Figure 1. Strontium carbonate strontium-87 NMR spectra: (A) static echo at 11.74 T, (B) static echo at 21.14 T, and (C) quadrupolar Carr-Purcell Meiboom-Gill (QCPMG) spectrum at 21.14 T.

Based on the observed enhancements in NMR signals from the crystalline strontium compounds, we intend to continue our investigations of strontium nuclei at EMSL and progress toward strontium detection in environmentally relevant clay minerals and zeolites. We will be returning in the spring of 2005 to perform magic angle spinning (MAS) strontium-87 NMR experiments on the crystalline samples, clays, and zeolites. MAS NMR enhances sensitivity by averaging the contribution of anisotropic first-order interactions, significantly reducing the line width. It is also our intent to return to EMSL in the summer of 2005 to attempt experiments that combine sensitivity-enhancing preparatory schemes with the QCPMG sequence. Rotor-assisted population transfer and double frequency sweep preparatory schemes further enhance the sensitivity of QCPMG experiments by saturating or inverting the outer transitions, thereby enhancing the population difference of the observed central transition (Schurko et al. 2003). We anticipate that these enhanced QCPMG methods will prove to be successful at detecting strontium in environmental samples.

References

Bastow TJ. 2002. "Electric Field Gradients at the M-Site in MCO_3: M=Mg, Ca, Sr, and Ba." *Chemical Physics Letters* 354(1-2):156-159.

Larsen FH, J Skibsted, HJ Jakobsen, and NC Nielsen. 2000. "Solid-State QCPMG NMR of Low-γ Quadrupolar Metal Nuclei in Natural Abundance." *Journal of the American Chemical Society* 122(29):7080-7086.

Schurko RW, I Hung, and CM Widdifield. 2003. "Signal Enhancement in NMR Spectra of Half-Integer Quadrupolar Nuclei Via DFS-QCPMG and RAPT-QCPMG Pulse Sequences." *Chemical Physics Letters* 379(1-2):1-10.

NMR Structural Investigations of the Breast Cancer Susceptibility Protein, BRCA1

P Brzovic,[(a)] DW Hoyt,[(b)] and RE Klevit[(a)]

(a) University of Washington, Seattle, Washington

(b) W.R. Wiley Environmental Molecular Sciences Laboratory, Richland, Washington

BRCA1 is a breast and ovarian cancer susceptibility protein that functions in critical cellular pathways. Our aim is to uncover and understand molecular factors that govern the assembly of BRCA1-mediated multiprotein complexes, including those involved in ubiquitination (when a protein is targeted for degredation). This work also aims to further our understanding of the molecular mechanisms underlying ubiquitination and unravel the deleterious structural and functional consequences of BRCA1 cancer predisposing mutations and their role in breast cancer cell biology.

The breast and ovarian cancer tumor suppressor protein BRCA1 is central to a number of fundamental cellular pathways. Its absence during embryogenesis is lethal. Loss of function in proliferating breast or ovarian epithelial cells can result in the development of cancer. BRCA1 has been shown to function in processes such as the cellular response to DNA damage, homologous recombination, transcriptional regulation, and more recently, ubiquitination. Protein ubiquitination provides a powerful regulatory mechanism for controlling pathways that include cell-cycle progression, transcriptional regulation, and responses to DNA damage. The importance of ubiquitin to cellular viablity is underscored by the 2004 Nobel Prize in Chemistry, awarded for research into the function of ubiquitination at the molecular level.

BRCA1 is a large and complicated protein undoubtedly composed of multiple functional domains. A growing body of literature suggests that BRCA1 interacts with at least 30 different macromolecules to accomplish its diverse functional roles. To date, our structural work has focused on the N-terminal Really Interesting New Gene (RING) domain of BRCA1 in complex with the N-terminal RING domain of BARD1. Of particular interest is the recent demonstration that the BRCA1 RING domain functions as a ubiquitin ligase, and interaction with the BARD1 RING domain is obligatory for this activity. As E3-ligases, RING domains are thought to facilitate the specificity of ubiquitination reactions by forming a multiprotein complex, binding both a ubiquitin conjugating enzyme (E2) covalently activated with ubiquitin and specific proteins targeted for ubiquitination. Cancer-predisposing mutations found in the BRCA1 RING domain have been found to interfere with its ability to function as a ubiquitin ligase. Thus, our research at W.R. Wiley Environmental Molecular Sciences Laboratory (EMSL) is poised to study two critical cellular pathways at the molecular level.

This system provides a unique opportunity for studying protein-protein interactions by nuclear magnetic resonance (NMR) spectroscopy. It involves characterizing the structures and interactions between at least four different protein components: BRCA1, BARD1, E2 (UbcH5c or UbcH7), and ubiquitin (Ub). The molecular weight of the fully assembled complexes approaches 60 kD. In previous years, we have been able to collect a great deal of

data on the individual components of this system. Over the last year, data collected on the 600-, 800-, and now 900-MHz instruments at EMSL have allowed us to develop a model of this multiprotein complex.

The first piece of the puzzle was determining of the solution structure of the BRCA1-BRCA1 RING domain heterodimer (Brzovic et al. 2001). Subsequently, we solved the NMR solution structure of UbcH5c. With these two structures in hand, we were able to investigate the complex formed between the BRCA1-BARD1 RING heterodimer and UbcH5c (Figure 1). Although other RING protein-E2 structures have been reported, this complex is catalytically competent, and the two proteins appear to associate in a manner substantially different from previous reports. These studies help to delineate factors that govern the specificity of RING(E3)-E2 protein interactions (Brzovic et al. 2003).

Figure 1. Structure of the BRCA1-BARD1 heterodimer (magenta) in complex with UbcH5c (blue-green). The UbcH5c active site cysteine is highlighted in yellow.

Second, our studies at EMSL uncovered a non-covalent binding site for Ub on a surface of UbcH5c located on a surface far removed from the active site. A single mutation in UbcH5c that disrupts this interaction is sufficient to eliminate BRCA1-directed poly-ubiquitin chain formation *in vitro*. Though the affinity of this site for Ub is low (Kd ~ 300 μM), data collection on both 800- and 900-MHz instruments at EMSL has been critical for calculating the structure of the UbcH5c-Ub structure (Figure 2.)

Figure 2. Structure of the non-covalent complex formed between UbcH5c and Ubiquitin. Ubiquitin (red) binds to the exposed β–sheet region of UbcH5c (blue-green). The active site of UbcH5c is on the opposite side of the molecule.

Recently, we have been able to generate and collect preliminary spectra on the activated UbcH5c~Ub covalent complex. In this complex, the C-terminus of Ub is covalently attached to the active site cysteine residue of UbcH5c via the formation of a thiolester bond. Surprisingly, with the exception of the extreme C-terminal tail of Ub, there are no other apparent interactions between UbcH5c and the attached Ub moiety.

These accomplishments allow us to build a model of an active BRCA1/BARD1 E3 ubiquitin-ligase complex (Figure 3). This is particularly exciting because these complexes have previously not been amenable to detailed structural characterization. The high-field NMR instrumentation available at EMSL made this work possible. We anticipate that during the coming year, these studies will help us further understand the complicated set of interactions between BRCA1 and its partner proteins.

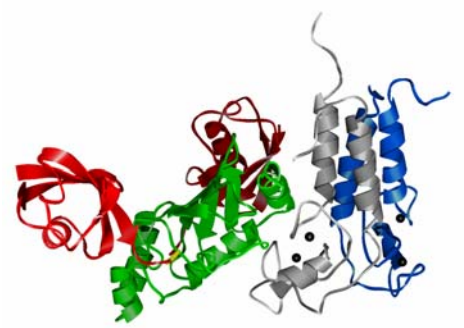

Figure 3. Assembly of an active ubiquitin-ligase complex involving BRCA1(gray)/ BARD1(blue), UbcH5c(green), and Ub (red).

Acknowledgements

We would like to ackowledge the help and assistance of EMSL staff members NG Isern and JJ Ford for their assistance with instrumentation and data collection.

References

Brzovic PS, P Rajagopal, DW Hoyt, MC King, and RE Klevit. 2001. "Structure of a BRCA1-BARD1 Heterodimeric RING-RING Complex." *Natural Structural Biology* 8(10):833-837.

Brzovic PS, JR Keeffe, H Nishikawa, K Miyamoto, D Fox, M Fukuda, T Ohta, and RE Klevit. 2003. "Binding and Recognition in the Assembly of an Active BRCA1-BARD1 Ubiquitin Ligase Complex." *Proceedings of the National Academy of Sciences* 100(10):5646-5651.

Protein Nuclear Magnetic Resonance Structures from the Northeast Structural Genomics Consortium in 2004

JR Cort,[a] TA Ramelot,[a] JM Aramini,[b] GJ Kornhaber,[b] DA Snyder,[b] MC Baran,[b] GVT Swapna,[b] AA Yee,[c] B Wu,[c] GT Montelione,[b] CH Arrowsmith,[c] and MA Kennedy[a]

(a) Pacific Northwest National Laboratory, Richland, Washington
(b) Center for Advanced Biotechnology and Medicine, Rutgers University, Piscataway, New Jersey
(c) University of Toronto, Toronto, Ontario, Canada

Protein structure and function are inextricably bound together. Structural genomics is a global effort to determine a representative sampling of high-resolution protein structures from all families of proteins.

Proteins comprise the machinery of the cell—they convert energy from one form to another, assemble and repair DNA, transmit signals from outside the cell to the nucleus, and serve countless other roles. For many proteins, roles have yet to be discovered. The large fraction of proteins that are functionally uncharacterized presents a major challenge for today's efforts to reach a holistic understanding of the cell, which typically contains thousands of different proteins. Knowledge of the structure of a particular protein of unknown function can aid the development and testing of hypotheses about its function. The collected knowledge of the structures of a representative sampling of all the proteins in the cell will enhance our ability to describe the cell as a networked system of interacting pieces, many of which are proteins.

The Northeast Structural Genomics Consortium (NESG) is a group of investigators at several institutions in the United States and Canada, funded by the Protein Structure Initiative of the National Institutes of Health and engaged in a project using both nuclear magnetic resonance (NMR) spectroscopy and x-ray crystallography for high-throughput protein structure determination. The W.R. Wiley Environmental Molecular Sciences Laboratory (EMSL) is one of several facilities at which NMR data are collected for NESG. These data are distributed to groups at Rutgers University, the University of Toronto, the State University of New York at Buffalo, and the Biological Sciences Division at Pacific Northwest National Laboratory. In 2004, complete data sets for nine proteins and partial data sets (usually select experiments at high field) for nine additional proteins were recorded for NESG. Full data sets typically represent 4 to 5 weeks of instrument time; the partial data sets take between 1 and 3 weeks of time. Altogether approximately 60 weeks of EMSL instrument time were devoted to structural genomics in 2004. Ten refined structures were deposited to the Protein Data Bank (PDB) at www.rcsb.org. Deposited structures (e.g, Powers et al. 2004, Ramelot et al. 2004) consist of atomic coordinates in cartesian space, though in Figure 1 they are shown as ribbon cartoon representations. These structures, which represent the final product produced from the data collected at EMSL, are available in the PDB for use by scientists everywhere.

Following structure determination, NESG scientists compare the structures to others in the structural database. Often, two proteins with dissimilar amino acid sequences that adopt similar structures will have functional similarities. Other clues to protein function can be

derived from identification of particular arrangements of amino acid side chains in the structure. Such analyses often suggest further experimental studies and can lead to new discoveries in biochemistry and molecular biology.

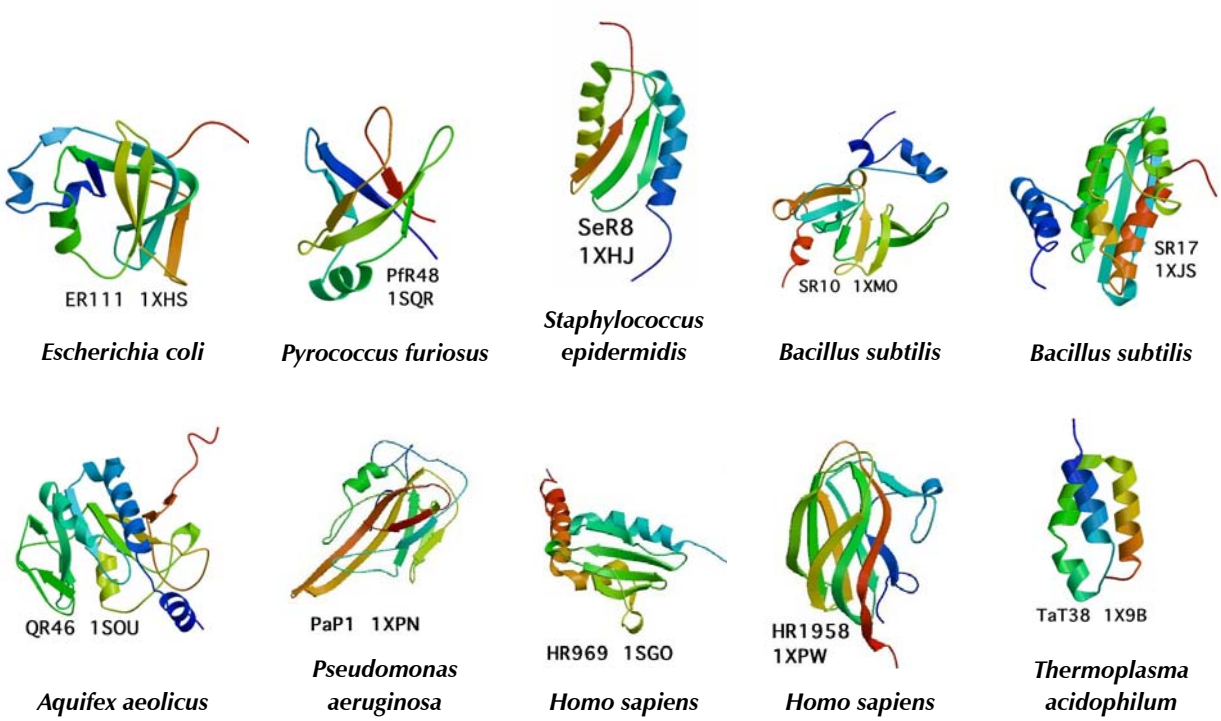

Figure 1. Structures of 10 proteins, determined with data collected at the EMSL High-Field Magnetic Resonance Facility for NESG. For each protein structure, the NESG and PDB identification numbers are given.

References

Powers R, TB Acton, Y Chiang, PK Rajan, JR Cort, MA Kennedy, J Liu, L Ma, B Rost, and GT Montelione. 2004. "^{1}H, ^{13}C and ^{15}N Assignments for the *Archaeglobus fulgidis* Protein AF2095." *Journal of Biomolecular NMR* 30(1):107-108.

Ramelot TA, JR Cort, S Goldsmith-Fischman, GJ Kornhaber, R Xiao, R Shastry, TB Acton, B Honig, GT Montelione, and MA Kennedy. 2004. "Solution NMR Structure of the Iron-Sulfur Cluster Assembly Protein U (IscU) with Zinc Bound at the Active Site." *Journal of Molecular Biology* 344(2):567-583.

Resolution of Aluminum-27 Nuclear Magnetic Resonances from Aluminosilicate Phases in Simulated Tank Waste Precipitates

GM Bowers,[(a)] S Choi,[(b)] J Chorover,[(b)] and KT Mueller[(a)]
(a) Pennsylvania State University, University Park, Pennsylvania
(b) University of Arizona, Tucson, Arizona

Isolation of the mineral phases present in simulated tank waste precipitates (analogous to those minerals precipitated from the soil solution during mineral weathering under near-field exposure to tank waste) using high-field ^{27}Al NMR will allow the formation kinetics for each precipitated mineral to be uniquely identified and help unravel the kinetic processes occurring in soils exposed to waste from leaking storage tanks.

An understanding of radio-cation mobility in the lithosphere and hydrosphere is necessary to predict the environmental fate of nuclides released from leaking storage tanks at U.S. Department of Energy sites such as the Hanford Site in Washington. The types of minerals present in the soil, their cation exchange capacities, and their affinities for various cations play important roles in cation transport. Clay minerals exposed to Hanford tank waste under near-field conditions have been shown to undergo mineral transformation reactions that produce tetrahedral aluminosilicate phases, thus complicating transport models with mineral dissolution and formation kinetics and by introducing new mineral phases to the soils (Chorover et al. 2003). While dissolution kinetics have been identified for a number of clays, there have been no direct kinetic studies of neo-formed precipitates under representative Hanford-like conditions. The overall goal of this project is to investigate the kinetics of precipitate formation and identify precipitates that sequester cesium, strontium, and iodine. We are using the solid-state nuclear magnetic resonance (NMR) capabilities at the W.R. Wiley Environmental Molecular Sciences Laboratory (EMSL) and complementary analysis techniques to achieve our goal.

Chorover and his team prepared precipitate phases from a simulated tank waste leachate solution (0.05-M $Al(OH)_4^-$, 2-M Na^+, 1-M NO_3^-, pH near 14, varying concentrations of Cs^+, Sr^{2+}, I^-) at room temperature and 60°C by seeding the solution with colloidal silica and collecting the precipitates as a function of exposure time to the simulated waste solution. This approach mimics the processes occurring within the soil solution that result in tetrahedral aluminosilicate formation in the environment, but avoids any complications caused by mineral weathering. The results of aluminum-27 magic angle spinning (MAS) NMR experiments on 30-day reacted precipitates at 9.4 T showed indications of multiple tetrahedral aluminosilicate phases that were poorly resolved. Aluminum-27 has a quadrupolar nucleus ($I = 5/2$); therefore, the width of each resonance decreases with increasing external field strength, improving resolution. We performed an identical set of aluminum-27 MAS NMR experiments on the 17.61-T instrument at EMSL in an attempt to resolve the resonances associated with each precipitated phase.

Our results at 17.61 T showed a substantial improvement in resolution over the MAS NMR at 9.4 T (Figure 1). Spectral results were fairly consistent within a parent solution silicon-to-aluminum ratio regardless of contaminant ion or concentration. None of the samples contained a significant amount of octahedrally coordinated aluminum, as was expected based on mineral dissolution studies. The 2:1 silicon-to-aluminum precipitate samples had four visible peaks in the tetrahedral aluminum region at 17.61 T, two well-separated resonances at 55 ppm and 65.5 ppm, and two overlapping resonances at approximately 60 and 61 ppm. The resonance at 55 ppm was not large and was not observable at field strengths below 17.61 T. The 1:1 silicon-to-aluminum precipitates were also shown to have four distinct resonances at 17.61 T, clearly resolved peaks at approximately 54.5 and 66 ppm, and two overlapping resonances at approximately 60 and 61 ppm. Results at 17.61 T also showed that the phases associated with the well-resolved peaks (approximately 55 and 65 ppm) were more abundant in the 1:1 silicon-to-aluminum precipitates than the 2:1 silicon-to-aluminum precipitates. The resolution of these four sites also allowed for an appropriate deconvolution of the 9.4-T data and calculation of the quadrupolar product and isotropic chemical shift for aluminum-27 nuclei in each aluminosilicate phase.

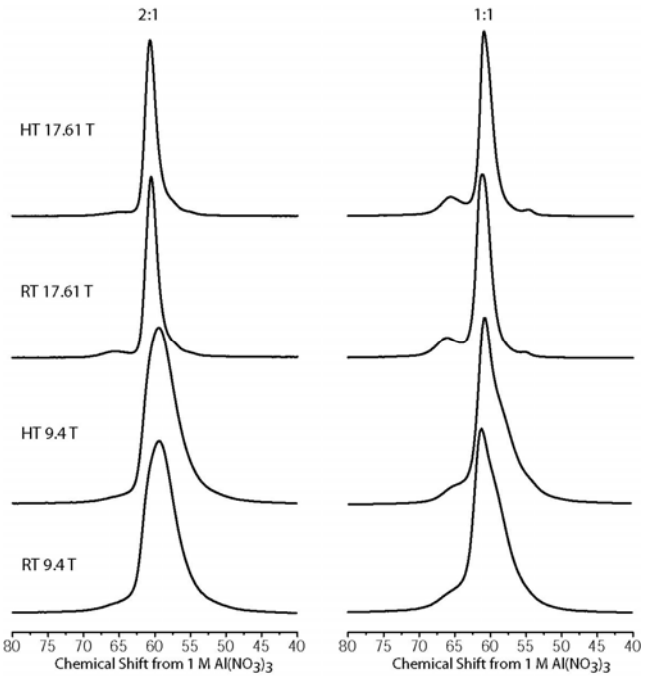

Figure 1. Comparison of aluminum-27 MAS NMR spectra for samples without contaminant ion. Spectra in bottom two rows from 9.4 T and top two rows from 17.61 T. The parent solution silicon-to-aluminum ratio is indicated at the top of each column and the reaction temperature (RT=room temperature, HT=60°C) on the left.

Reaction temperature appeared to play a small role in the precipitate formation kinetics. The 17.61-T results show that precipitates collected from room-temperature simulated tank waste leachate solution have peaks that are shifted slightly downfield in the 2:1 and 1:1 silicon-to-aluminum precipitates vs. the heated samples. The peak at approximately 65 ppm in the 2:1 silicon-to-aluminum precipitates is more prevalent in the room-temperature samples than those collected from the heated reaction mixture. The ratio of the 60 ppm resonance to the 61 ppm resonance also varies slightly in the 1:1 silicon-to-aluminum precipitates between the two temperatures.

Reference

Chorover J, S Choi, MK Amistadi, KG Karthikeyan, G Crosson, and KT Mueller. 2003. "Linking Cesium and Strontium Uptake to Kaolinite Weathering in Simulated Tank Waste Leachate." *Environmental Science Technology* 37(10):2200-2208.

Solution Structure of the Conserved Hypothetical Protein Rv2302 from the Bacterium *Mycobacterium tuberculosis*

GW Buchko,[(a)] CY Kim,[(b)] TC Terwilliger,[(b)] and MA Kennedy[(a)]

(a) Pacific Northwest National Laboratory, Richland, Washington

(b) Los Alamos National Laboratory, Los Alamos, New Mexico

Determining the structure and function of hypothetical proteins from the bacterium responsible for tuberculosis, Mycobacterium tuberculosis*, may lead to the development of new therapies and strategies to combat this deadly disease.*

Mycobacterium tuberculosis is the aetiological agent responsible for the chronic infectious disease tuberculosis. Countless millions of people have died from tuberculosis and this gram-positive tubercle bacillus continues to claim more lives worldwide than any other infectious agent, despite the availability of effective short-term chemotherapy and extensive vaccinations. Indeed, there has been a recent increase in the incidents of tuberculosis in both developing and industrialized nations as new drug-resistant strains have emerged, and a deadly synergy with human immunodeficiency virus has evolved. Recently, the complete genome of *M. tuberculosis* has been sequenced. A Tuberculosis Structural Genomics Consortium has been established with the goal of using the genomic information to discover and analyze the structures of more than 400 proteins from *M. tuberculosis*. In addition to providing a foundation for a fundamental understanding of biology, the information and knowledge obtained from determining the structures of the proteins in the *M. tuberculosis* genome will facilitate the conception and development of new therapies and strategies to treat and control this lethal disease. In pursuit of these goals, we have determined the solution structure for the highly conserved *M. tuberculosis* protein Rv2302 using nuclear magnetic resonance (NMR)-based methods.

Rv2302 is a small 8.6 kDa protein of 80 amino acids. Using a suite of three- and four-dimensional NMR experiments collected on medium-field magnets at EMSL, the majority of the backbone and side chain proton, carbon, and nitrogen resonances for Rv2302 were assigned. Figure 1 shows the ^{1}H-^{15}N heteronuclear single quantum correlation (HSQC) spectrum for Rv2302 with the assigned cross peaks for the ^{1}HN amide resonances labeled. Unassigned cross peaks are labeled with a question mark (?)

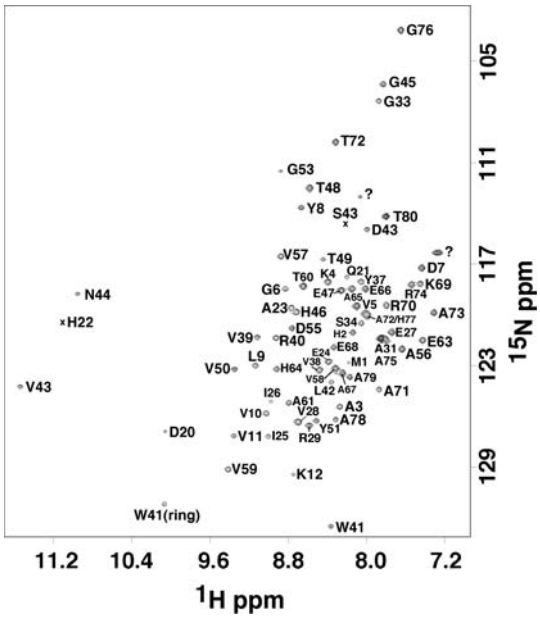

Figure 1. ^{1}H-^{15}N HSQC spectrum of Rv2302.

and weak cross peaks are labeled with an 'x.' Data were collected at 25°C in an NMR buffer (100-mM potassium chloride, 20-mM potassium phosphate, 2.0-mM dithiothreitol, pH 7.1) at a ^{1}H frequency of 600 MHz. Aside from a stretch of seven residues between G13 to H19, all the backbone amide resonances were assigned. Note that even before collecting the three- and four-dimensional NMR data, the wide chemical shift dispersion observed in both the nitrogen and proton dimension in the ^{1}H-^{15}N HSQC spectrum indicated that Rv2302 was structured in solution.

Distance restraint files were generated using nuclear Overhauser effect (NOE) data extracted from three-dimensional ^{15}N and four-dimensional ^{13}C-filtered nuclear Overhauser effect spectroscopy (NOESY) experiments. A hydrogen bond distance restraint file was extracted from deuterium exchange data and a dihedral angle restraint file generated from a combination of chemical shift index analysis of chemical shifts, NOESY data, and torsional angle likihood obtained from shift calculations. Figure 2 shows two views of the calculated structure that most closely superimposed on the average structure of the latest 15/30 lowest energy structures generated by the nih_xplor software.

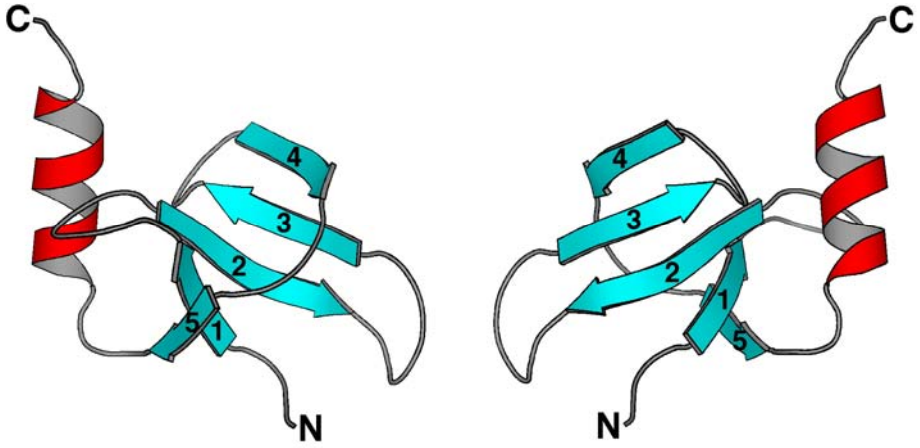

Figure 2. Molscript representation of the preliminary solution structure determined for Rv2302. The structures differ by a 180° rotation about the vertical axis.

The protein is composed of a five-strand, anti-parallel β-sheet with a 10 residue α-helix nestled onto one side of the β-sheet. Initial Dali searches do not produce any significant hits, suggesting that the fold for Rv2302 may be novel. Because the biological function of Rv2302 is still unknown, we are currently screening the protein to elucidate activity. Once a potential function is identified it will be possible to probe potential substrates through the technique of chemical shift mapping. The technique is based on the premise that protein-ligand interactions usually perturb the chemical environment of the nuclei at the interface of ligand binding. Such perturbations are often accompanied by changes in the chemical shifts of the backbone ^{1}HN and ^{15}N resonances (the ^{1}H-^{15}N HSQC spectrum shown in Figure 1). By identifying resonances that undergo a binding-dependent chemical shift or intensity perturbation, it is possible to identify ligands that bind to a protein and to map the location of the ligand binding site onto the three-dimensional structure of the protein. If Rv2302 is revealed to play an important role in this lethal bacterium's life cycle, then similar chemical shift mapping experiments may be used to find a substrate that turns this protein 'off' to kill the bacterium.

Structure of the Serine-Rich Domain from Crk-Associated Substrate (p130Cas)

K Briknarová,[(a)] F Nasertorabi,[(a)] ML Havert,[(a)] DW Hoyt,[(b)] K Vuori,[(a)] and KR Ely[(a)]

(a) Burnham Institute, La Jolla, California

(b) W.R. Wiley Environmental Molecular Sciences Laboratory, Richland, Washington

This is the first reported structure of the serine-rich, protein-interaction motif that is found in the Cas family of docking proteins. This study helps understand how cells adhere to each other, which is related to the spread of tumors to other parts of the body.

Focal adhesions are multiprotein signaling complexes that form at the sites of integrin-mediated contact between cells and the extracellular matrix (ECM). They physically link the ECM with the cytoskeleton and transduce signals between the ECM and the cytosol. The docking protein p130Cas (Cas; Crk-associated substrate) is involved in assembly of focal adhesions and concomitant cellular signaling. Cas plays a role in physiological regulation of cell adhesion, migration, survival, and proliferation, as well as in oncogenic transformation. It consists of multiple protein-protein interaction motifs including a serine-rich region that is positioned between Crk and Src-binding sites. We acquired nuclear magnetic resonance (NMR) data using research capabilities available in the W.R. Wiley Environmental Molecular Sciences Laboratory (EMSL) and solved the structure of the serine-rich region.

This domain, approximately 160 residues long, is highly helical and exhibits rather degenerate chemical shifts (Figure 1). Hence, it presented a challenge for nuclear Overhauser effect spectroscopy assignment and structure determination. Also, while we had assigned most of the backbone resonances using standard triple resonance experiments and uniformly

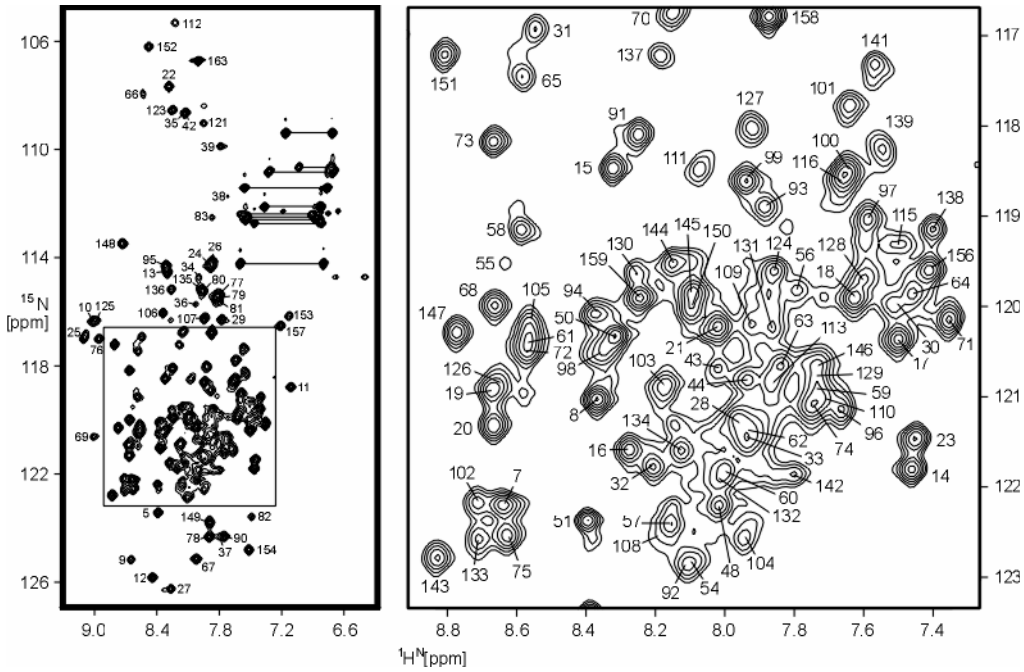

Figure 1. ^{1}H-^{15}N Heteronuclear single quantum correlation spectrum of the serine-rich domain from p130Cas. The crowded central region is shown expanded in the right panel.

carbon-13/nitrogen-15-labeled protein samples, side chain assignment proved difficult since signals from many γ, δ, and ε atoms were not observed in the C(CO)NH and H(CCO)NH spectra. Hence, to complete the side-chain assignment, we acquired C(CO)NH and H(CCO)NH experiments for a fractionally deuterated sample. We also recorded four-dimensional carbon-13/nitrogen-15 NOESY experiments to obtain less ambiguous distance restraints for structure calculation. At the time, only a three-channel, 500-MHz NMR spectrometer was available at the Burnham Institute. Access to four-channel spectrometers at EMSL was essential for experiments with the fractionally deuterated sample, and all experiments greatly benefited from data acquisition at higher field to improve resolution and relieve spectral overlap.

The structure identified in this research represents the first molecular model for the serine-rich sequence motif from Cas family proteins. It comprises a four-helix bundle (Figure 2)—a structural building block that is also employed to mediate protein-protein interactions by other components of focal adhesions and adherens junctions, such as focal adhesion kinase, α-catenin, and vinculin. The serine-rich region may mediate protein-protein interactions in a similar manner. Mapping the degree of amino acid conservation onto the molecular surface implies a patch of highly invariant residues close to the C-terminus of the domain in interaction with another protein yet to be identified.

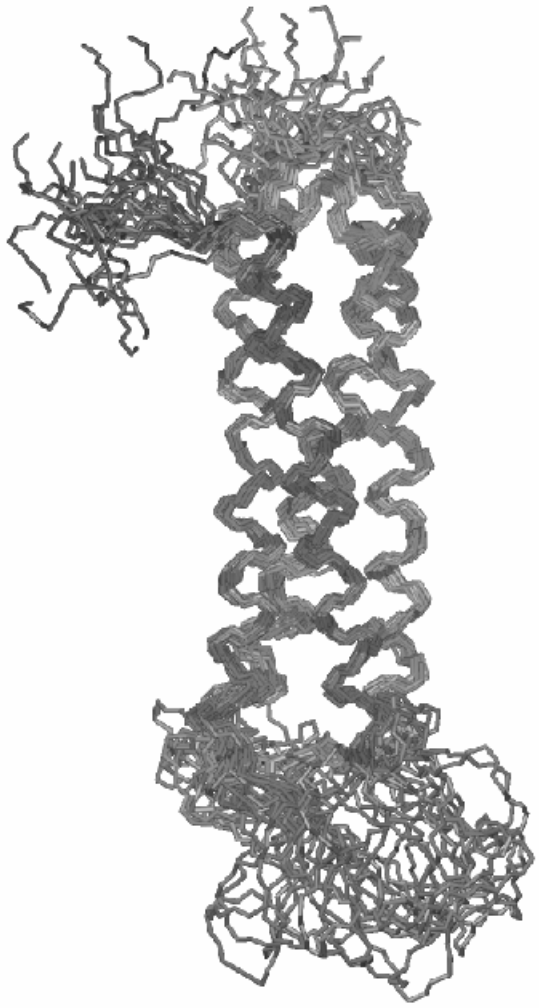

Figure 2. Twenty backbone traces of the serine-rich domain of p130Cas are shown superimposed in their α-helical regions.

Structure of Telomerase and Telomeric Proteins

T Leeper,[(a)] SL Reichow,[(a)] Y Chen,[(a)] JK Fender,[(a)] KS Godin,[(a)] and G Varani[(a)]
(a) University of Washington, Seattle, Washington

The study of the structure of telomerase ribonucleic acid and its associated protein would lead to an understanding of how the genetic integrity of a chromosome is retained during cell division and to a possible new avenue to cancer treatment.

Telomerase is the ribonucleoprotein (RNP) enzyme responsible in most eukaryotes for the replication of the chromosome termini (telomeres). It also plays a critical role in cellular division and cancer; it is activated in the germ line and in the great majority of cancer cells. In humans, it is composed of a 400-nucleotide ribonucleic acid (RNA) and several proteins that associate with it. It carries out the enzymatic activity and promotes its cellular localization and assembly. We are studying the structure of two critical domains of telomerase RNA responsible for RNA biogenesis and for recruitment of the catalytic activity to the holoenzyme, respectively. Four proteins of unknown structure bind to human telomerase RNA; in doing so, these proteins stabilize the RNA in the cell and direct its processing and nuclear localization. We aim to determine the structures of two such proteins (called Nop10 and Gar1) and of their associated RNA domains. Nuclear magnetic resonance (NMR) studies conducted at the University of Washington and the W.R. Wiley Environmental Molecular Sciences Laboratory (EMSL) have provided very high-quality data for the proteins and for a key domain of human and lower eukaryotic telomerase RNAs. NMR experiments conducted at EMSL contributed significantly to our progress towards determining the structures of critical domains of human telomerase RNA and its associated proteins.

Nop10 plays an essential function in the biogenesis of telomerase and of the ribosome. NMR spectra of very high quality, collected in part at EMSL, have allowed us to determine the structure of the archeal and yeast proteins (Figure 1). The archeal protein forms a zinc-knuckle packed against a C-terminal helix. The yeast and human proteins have lost the zinc-binding domain, but yNop10 retains a similar overall fold, though with considerably increased flexibility. Data collected at EMSL are also allowing structure determination of the archeal and yeast Gar1 proteins. Because of high levels of sequence homology, the structure of the human protein will be reliably modeled once these studies are completed. Although it was thought to be related to

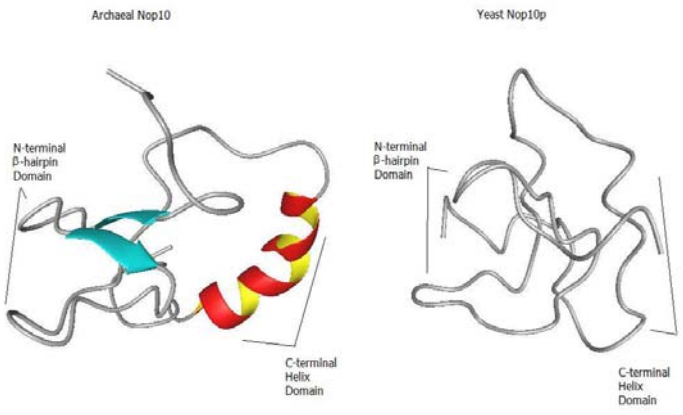

Figure 1. NMR structures of archea (left) and yeast (right) Nop10 proteins determined in part using data collected at EMSL.

Sm proteins, a family of RNA-binding protein that form ring-like structures on U-rich RNAs, Gar1 forms an all-β structure of different fold.

Human and mouse telomerase RNAs retain a domain called CR4-CR5 that is capable of reconstituting telomerase activity when combined with the template domain. It is a key functional element of vertebrate telomerases that we hypothesize is conserved in all eukaryotes, including ciliates. The NMR work on the human CR4/CR5 domain conducted at EMSL has progressed as shown in Figure 2. The P6.1 stem-loop interacts with the template domain and promotes the tertiary folding of the RNA and perhaps even participates in catalysis. Completion of the structure will provide unprecedented insight into the structure-function of this key eukaryotic enzyme. At the same time, we have collected data on a domain from ciliate telomerases that we hypothesize is functionally equivalent. We hope that the structural comparison will help shed light on the detailed mechanism of action of these RNAs.

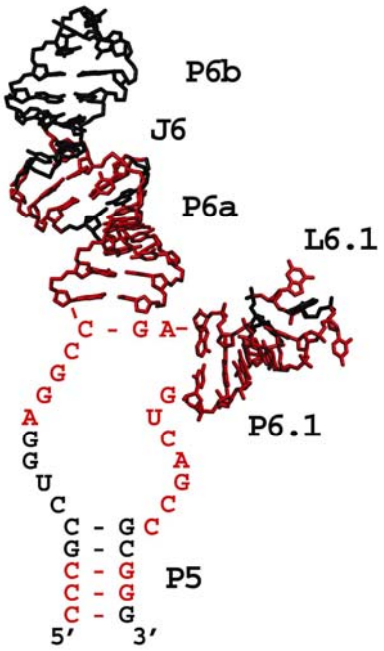

Figure 2. Current progress in the structure determination of the domain of human telomerase RNA responsible for activation of the enzymatic activity.

The NMR data gathered to date have provided key information for spectral assignments and collection of structural constraints. They have also allowed the optimization of constructs and purification/sample conditions.

Study of the Binding of Salivary Peptide Fragment SN-15 to Hydroxyapatite Using $^{15}N\{^{31}P\}$ REDOR

V Raghunathan,[(a)] JM Gibson,[(a)] JM Popham,[(a)] PS Stayton,[(a)] and GP Drobny[(a)]
(a) University of Washington, Seattle, Washington

This study may contribute to a better understanding of the crystal recognition mechanisms employed by proteins and peptides that are involved in the regulation of biomineralization. Advances in controlling biomineralization can lead to improved binding of bone to metal or ceramic artificial devices.

Molecular recognition mechanisms used by proteins to control biomineralization processes are of considerable interest because the knowledge gained would allow for the design of biomimetic peptide coatings for biomaterial and tissue engineering applications. Acidic proteins found in mineralized tissues act as nature's crystal engineers, where they play a key role in promoting or inhibiting the growth of minerals such as hydroxyapatite (HAP), the main mineral component of bone and teeth. Despite their importance to dentistry, there is remarkably little known of the protein structure-function relationships governing hard-tissue engineering. Among the acidic proteins found in the saliva is statherin, a 43 amino-acid tyrosine-rich peptide that is an inhibitor of both HAP crystal growth and nucleation. We used $^{15}N\{^{31}P\}$ rotational-echo, double-resonance (REDOR) nuclear magnetic resonance (NMR) spectroscopy (Gullion and Schaefer 1989) to analyze the binding mechanism of a 15 amino-acid fragment of statherin (SN-15) to the HAP surface. By using $^{15}N\{^{31}P\}$ REDOR and $^{13}C\{^{31}P\}$REDOR to measure the distance from either a carbon atom or nitrogen atom of the peptide to a phosphorus atom on the HAP surface, we gain insight into the binding motif. A diagram of the proposed and already-used labels is shown in Figure 1. SN-15 has already been shown to be helical in nature (Long et al. 2001), and by determining which side-chains interact with the surface, we can determine the orientation of the helix. The first REDOR experiment involved measuring the distance from the lysine side-chain to the HAP surface.

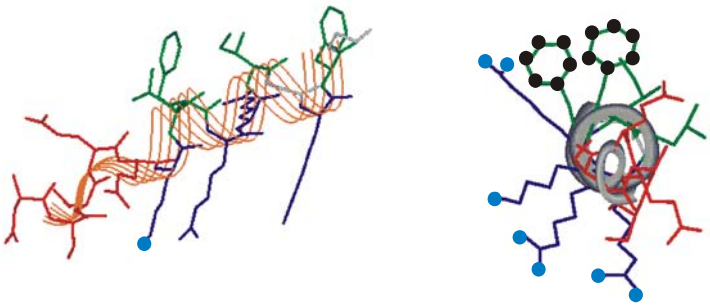

Figure 1. Views from the side and end of the SN-15 peptide showing probable locations of the side-chains on the SN-15 helix. The side view on the left shows the lysine label used in the experiment described here, whereas the end view on the right shows all the labels we anticipate using in future REDOR experiments. Labeled ^{15}N atoms are in blue, and labeled ^{13}C atoms are in black. Each side-chain is labeled independently for individual REDOR experiments.

REDOR is designed to measure the distance between a pair of atoms with no other NMR active nuclei nearby. SN-15 has phosphoserine side-chains near the lysine that complicate

the measurements. Results from lyophilized samples suggested a perturbation of the structure near the ^{15}N side-chain of the Lysine-6 residue caused by the presence of the surface compared to the free peptide. More biologically relevant experiments requiring hydrated conditions were performed at the W.R. Wiley Environmental Molecular Sciences Laboratory (EMSL). These data are shown in Figure 2. Since the peptide interacts with several phosphorus atoms on the surface, which also interact with the phosphoserine side-chain, it becomes difficult to fit the data quantitatively to what is predicted. It is not known how many phosphorus atoms are interacting in the spin system and whether the ^{15}N K6 side-chain is interacting directly with several phosphorus surface atoms or the phosphorous in the phosphoserine side-chain. This puzzle will be solved in the near future using alternate samples that eliminate the interference problem.

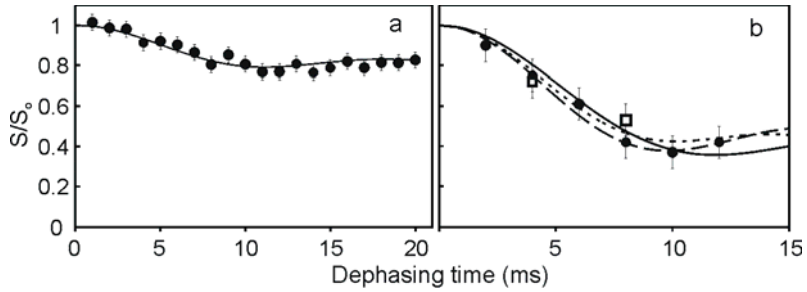

Figure 2. (a) $^{15}N\{^{31}P\}$ REDOR was performed on an unbound SN-15 sample to assess the likelihood of interference from the phosphoserine side-chain. A best-fit scenario with 80% of the K6 ^{15}N spins away from the ^{31}P spins and 20% of the K6 ^{15}N spins 3.2 Å from a ^{31}P spin fit the data. (b) $^{15}N\{^{31}P\}$ REDOR was also performed on a SN-15 sample bound to HAP. The circles are experimental data from the lyophilized SN-15 bound to HAP, while the squares are experimental data from the hydrated sample. Three possible models that fit our REDOR data are shown. The solid line represents a system where the K6 ^{15}N is 3.7 Å from one ^{31}P spin and 4.4 Å from a second with the two ^{31}P spins being 2.2 Å apart. The long dashed line represents the system where a bimodal distribution exists; 40% of the ^{15}N K6 spin remain uncoupled and 60% are 3.1 Å from a ^{31}P spin. The short dashed line represents a system that is nearly linear in its geometry with ^{15}N-^{31}P distances of 3.7 Å and 4.0 Å.

References

Gullion T and J Schaefer. 1989. "Rotational-Echo Double-Resonance NMR" *Journal of Magnetic Resonance* 81(1):196-200.

Long JR, WJ Shaw, PS Stayton, and GP Drobny. 2001. "Structure and Dynamics of Hydrated Statherin on Hydroxyapatite as Determined by Solid-State NMR." *Biochemistry* 40(51):15451-15455.

The Juxtamembrane Domain of the Epidermal Growth Factor Receptor

K Choowongkomon,[(a,b)] C Carlin,[(a,b)] and FD Sönnichsen[(a,b)]

(a) Case Western Reserve University, Cleveland, Ohio

(b) Center for Autosomal Recessive Polycystic Kidney Disease, Rainbow Children's Hospital, Cleveland, Ohio

Growth factor-receptor complex formation translates into a signal across a membrane to initiate biological processes within a cell. In particular, understanding the structure-function relationship at the juxtamembrane domain will help understand the receptor's role in cancer and kidney disease.

The epidermal growth factor receptor (EGFR) is the prototypic member of the tyrosine kinase receptor family that comprises four receptors: EGFR (or ErbB1), ErbB2, ErbB3, and ErbB4 (Wells 1999). EGFR is widely expressed in many cell types, including epithelial and mesenchymal lineages. Upon binding at least five distinct ligands, EGFR dimerizes, leading to the activation of its intrinsic kinase domain and the phosphorylation of itself and numerous intermediary effector molecules. This initiates several signaling pathways that cause important biological responses such as mitogenesis or apoptosis, enhanced cell motility, protein secretion, and differentiation or de-differentiation. In addition to being implicated in organ morphogenesis, maintenance, and repair, up-regulated EGFR signaling has been correlated with a wide variety of tumors, and EGFR misregulation has been shown to be a hallmark of polycystic kidney disease.

EGFR is composed of a large extracellular domain, a single-helix transmembrane region, a juxtamembrane domain, and a cytosolic kinase domain. Its activity is tightly regulated by compartmentalization and by ligand-induced endocytosis. These processes are governed by sorting signals, short amino acid sequence motifs, which are found in the juxta-membrane domain located between the transmem-brane helix and the tyrosine kinase domain. We are studying the structure-function relationship of the sorting signals in receptor localization and trafficking as well as in the regulation and expression of this receptor during cell differentiation and polarization.

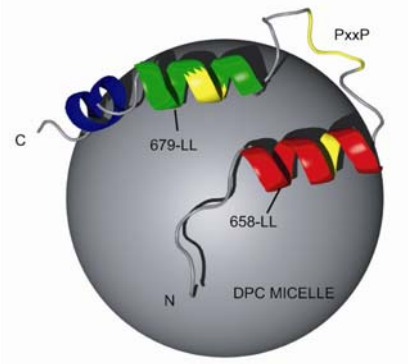

Figure 1. Ribbon presentation of a model of the detergent micelle-bound JX domain of EGFR as determined by solution nuclear magnetic resonance (NMR) spectroscopy. The three sorting signals are highlighted in yellow.

The structural characterization of the entire, isolated juxtamembrane region of EGFR has been completed by NMR spectroscopy, and particularly using the data acquired at the ultrahigh-field instruments at the W.R. Wiley Environmental Molecular Sciences Laboratory (Choowongkomon et al. 2004). To delineate how the environmental context alters the structure of the region and the accessibility of the encompassed signaling sequences, the studies were performed in the presence of detergent micelles, which mimic the native environment of the receptor domain (Figure 1). The peptide is nearly 100% detergent-micelle bound as shown by diffusion experiments. Chemical shift assignments have been

completed, using both singly as well as doubly labeled protein. Structural information was obtained first from heteronuclear edited nuclear Overhauser effect spectroscopy (NOESY) experiments. Additional valuable information included residual dipolar couplings obtained in stretched acrylamide gel, hydrogen bond information from hydrogen/deuterium exchange, relaxation data, and orientational information derived from differential broadening effects of spin-labeled detergent.

Combined, these data characterize three distinct helical regions, which are surface associated with the detergent micelle surface. All unambiguously assignable nuclear Overhauser effects in both ^{15}N- and ^{13}C-edited NOESY experiments are either short or medium range. No distance information was obtained that defines the spatial relationship between helices 1 and 2. Helices 2 and 3, however, are linked by several restraints and are separated by a defined two-residue kink. A common hydrophobic surface created on one side of these helices has been shown (by relaxation broadening studies) to comprise the micelle-surface binding site. Two of these helices encompass the dileucine basolateral and lysosomal signal sequences. The side-chains of these signals are located in the hydrophobic face of the helices and, thus, are embedded in the micelle surface. Only the third sorting signal, a basolateral signal composed of the novel PxxP motif, links helices 1 and 2. This linker is conformationally flexible and is not associated with the detergent micelle. And, foremost, it remains accessible. This structure highlights the differential properties of the sorting signals and suggests that the dominance of the basolateral sorting signal is correlated with its high accessibility. It also indicates that a specific secondary structure is not required for recognition of this signal and that its binding specificity to the sorting machinery is encoded in its primary sequence.

References

Choowongkomon K, ME Hobert, C He, C Carlin, and FD Sönnichsen. 2004. "Aqueous and Micelle-Bound Structure of the Epidermal Growth Factor Receptor Juxtamembrane Domain Containing Basolateral Sorting Motifs." *Journal of Biomolecular Structure and Dynamics* 21(6):813-826.

Wells A. 1999. "EGF Receptor." *International Journal of Biochemistry and Cell Biology* 31(6):637-643.

Using Nuclear Magnetic Resonance Spectroscopy to Unravel the Structural Details of Enhanceosomes: Transcription-Enhancing Complexes

GW Buchko,[(a)] K McAteer,[(b)] S Ni,[(a)] R Reeves,[(c)] and MA Kennedy[(a)]

(a) Pacific Northwest National Laboratory, Richland, Washington
(b) Washington State University Tri-cities, Richland, Washington
(c) Washington State University, Pullman, Washington

Knowing the structural details of the enhanceosome at the molecular level could open the door to new chemotherapy treatments for various forms of cancer. Enhanceosomes provide the architectural framework for protein binding, setting the stage for DNA replication.

The non-histone chromatin-associated high-mobility group HMGA1 proteins regulate expression of numerous genes *in vivo* by participating in transcription-enhancer complexes known as enhanceosomes (Figure 1). While HMGA1 is barely expressed in normal adult tissue, expression levels are elevated in tumors, suggesting that alterations in the HMGA1 gene could play an important role in the generation of benign or malignant tumors. These 'architectural' transcription factors recognize DNA structure rather than sequence, binding to the minor groove of AT-rich promoter sequences. HMGA1 is also known to bind directly with more than a half a dozen other transcription factors in various enhanceosomes. Circular dichroism and nuclear magnetic resonance (NMR) studies indicate that HMGA1 lacks secondary or tertiary structure when free in solution. When HMGA1 binds DNA, a unique secondary structure referred to as an "AT-hook" is induced in the DNA binding regions. HMGA1 contains three AT-hooks, similar in sequence but independent, flanked by positively charged lysine and arginine residues. Our limited molecular-level understanding of how HMGA1 binds DNA comes from a single structure of a truncated HMGA1 containing only two AT-hooks (HMGA1[2/3]) bound to two different DNA dodecamers, which was solved using NMR spectroscopy. With the truncated HMGA1(2/3) and short DNA, which contained just a single AT-hook binding site, the structure and dynamics of the linkers could not be characterized. Additionally, because of the short length of the DNA oligomer, the impact of HMGA1 binding on DNA curvature, especially any coherent bending caused by multiple AT-hooks, could not be examined. There have been several advances in NMR technology since the earlier HMGA1 structure was published, including increases in field strength (such as the 21.1-Tesla magnet at the W.R. Wiley Environmental Molecular Sciences Laboratory), more powerful NMR experiments, and more versatile DNA and protein labeling capabilities.

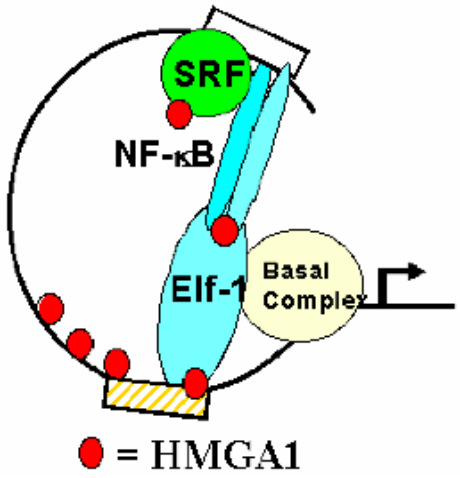

Figure 1. Schematic model of an enhanceosome formed with Elf-1. It is believed that HMGA1 bends the DNA to allow other proteins, such as Elf-1, NF-kB, and SRF, to interact.

Using these tools, we are examining a fragment of HMGA1a containing all three AT-hooks (HMGA92: residues 1-92) bound to a DNA molecule long enough to accommodate all three AT-hooks (MS15 = d(CTCAAATATTTAAATAAACAG)) and a DNA molecule containing just one AT-hook (E20 = d(GCACACTTCCTATATTTGAG)) to advance our understanding of how HMGA1 becomes integrated into enhanceosomes.

Figure 2 shows the aromatic-to-H1' region of E20 free in solution (A) and in a 1:1 complex with HMGA92 that is ^{2}H-, ^{13}C-, and ^{15}N-labeled (B). The major observation is that the spectrum of free E20 (A), a 20 base-pair DNA duplex, is fully resolved at a ^{1}H resonance frequency of 900 MHz, indicating that it is possible to use NMR spectroscopy at this field strength to determine structures for DNA of this size. The fingerprint region of the spectrum shown has been completely assigned. Other major observations are that after the addition of a 1:1 molar equivalent of HMGA92 (B), 1) the same region of the spectrum is still well resolved, 2) a large subset of resonances are broader, and 3) many of the resonances shift. The observation that a subset of resonances becomes broader is expected, because complex formation increases the molecular weight of the DNA by approximately 10 kDa. Indeed, it was necessary to collect the data at 40°C to obtain the best spectral resolution. The observation that many of the resonances in the aromatic-to-H1' region shift after binding to the protein suggests that protein binding altered the structure of the DNA, because these chemicals shifts are sensitive to their molecular environment. Similar well-resolved spectra have been acquired for the MS15/HMGA92 complex; however, for this complex, it was necessary to collect the data at 55°C, presumably because MS15, with three consecutive AT-hook binding sites, binds more tightly to all the AT-hooks on HMGA92. Given the high quality of the spectra for the DNA alone and the DNA/protein complexes, isotopically labeled DNA is currently being synthesized to collect residual dipolar coupling data necessary to calculate meaningful DNA structures.

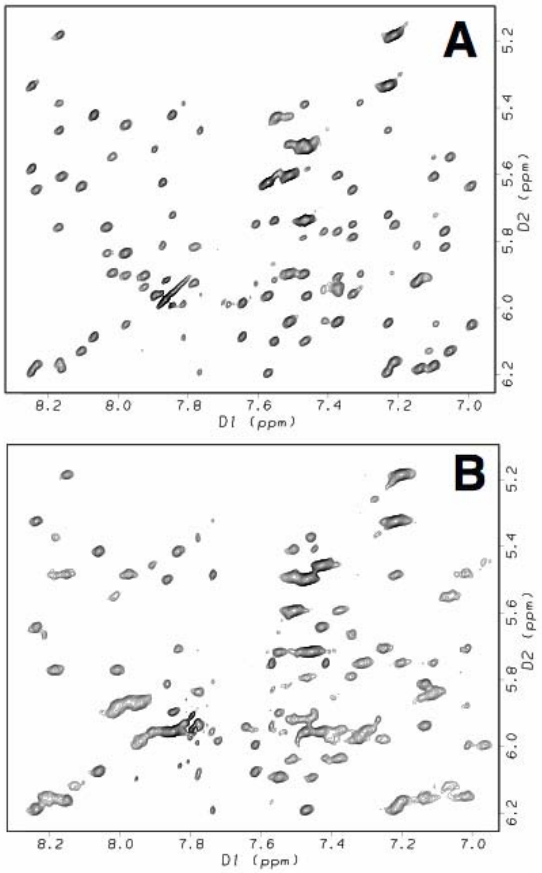

Figure 2. ^{1}H-^{1}H nuclear Overhauser effect spectroscopy spectra of E20 free in solution A) and in a 1:1 complex with ^{2}H-, ^{13}C-, ^{15}N-labeled HMGA92 B). Spectra were collected at a ^{1}H resonance frequency of 900 MHz at 40°C.

User Projects

High-Field Aluminum-27 Nuclear Magnetic Resonance Studies of Simulated Tank Waste Precipitates
GM Bowers, KT Mueller, GS Crosson
Pennsylvania State University, University Park, Pennsylvania

Application for 800-MHz Nuclear Magnetic Resonance Spectrometer Time to Facilitate the Structural Study of the Complex Formed by Poxvirus Encoded Protein vCCI and Human CC Chemokine MIP-1Beta
PJ Liwang, L Zhang
Texas A&M University, College Station, Texas

AlphaB-Crystallin: The Core and the Oligomer – A Structural Investigation
P Rajagopal, RE Klevit
University of Washington, Seattle, Washington

Characterization of the Structure of the Calcium-Dependent Antibiotic Daptomycin Using Solution-State and Solid-State Nuclear Magnetic Resonance Spectrometry
SK Straus, PC Dave
University of British Columbia, Vancouver, British Columbia, Canada

Determination of the Three-Dimensional Solution Structure of NosL: A Potentially Novel Copper (I) Metal Transporter
V Copie, LM Taubner
Montana State University, Bozeman, Montana

Structure and Interactions of a Domain of Dynein Intermediate Chain: Protein Folding Coupled to Binding
EJ Barbar
Oregon State University, Corvallis, Oregon

Structure Determination of Membrane Proteins
JL Mills, FD Soennichsen, K Choowongkomon
Case Western Reserve University, Cleveland, Ohio

Slow Magic-Angle Spinning of Lipids in Mouse Fast- and Slow-Skeletal Muscle
MJ Kushmerick, KE Conley, EG Shankland, D Lee
University of Washington, Seattle, Washington

Nuclear Magnetic Resonance Study of Circadian Clock Protein KaiA
Y Kim, AC Liwang
Texas A&M University, College Station, Texas

Hydrogen Storage Materials
WJ Shaw
Pacific Northwest National Laboratory, Richland, Washington

Study of the Binding Mechanism of Mutant SN-15 to Hydroxyapatite Using $^{15}N\{^{31}P\}$REDOR
JM Popham, V Raghunathan, JM Gibson, GP Drobny, PS Stayton
University of Washington, Seattle, Washington

Routine Hydrogen-1 and Carbon-13 Nuclear Magnetic Resonance Analysis of Functionalized Semiconductor and Metallic Nanoparticles Synthesized for Biodetection Studies
MG Warner, CJ Bruckner-Lea, JW Grate
Pacific Northwest National Laboratory, Richland, Washington

Nuclear Magnetic Resonance Structural Studies of Clustered DNA Damage
K McAteer, JH Miller
Washington State University, Richland, Washington
GW Buchko, MA Kennedy
Pacific Northwest National Laboratory, Richland, Washington

Structural Investigations of Solid Materials by High-Resolution, Solid-State Nuclear Magnetic Resonance at Very High Field
CA Fyfe, CM Schneider
University of British Columbia, Vancouver, British Columbia, Canada

Structural Determination of Apolipoprotein A-I/Preb-HDL Particles
J Wang, C Xu, X Ren, AP Sivashanmugam
Southern Illinois University, Carbondale, Illinois

Structural Studies of Lipid-Free Apolipoprotein A-I
J Wang, X Ren, AP Sivashanmugam, L Zhao
Southern Illinois University, Carbondale, Illinois

Correlation of Structure and Function of Zinc Metalloproteins Via Solid-State Nuclear Magnetic Resonance Methods
AS Lipton, PD Ellis, RW Heck
Pacific Northwest National Laboratory, Richland, Washington

Investigation of the Role of Mg^{2+} in DNA Repair Proteins APE1, Polþ, and FEN1
AS Lipton, PD Ellis, RW Heck
Pacific Northwest National Laboratory, Richland, Washington
DM Wilson
National Institute on Aging, Baltimore, Maryland
SH Wilson
National Institute of Environmental Health Sciences, Research Triangle Park, North Carolina

Investigation of Catalyst Reaction Mechanisms by *In Situ* High-Field, High-Resolution Nuclear Magnetic Resonance Spectroscopy
JZ Hu
Pacific Northwest National Laboratory, Richland, Washington

Structural Genomics Collaborative Access Team
MA Kennedy
Pacific Northwest National Laboratory, Richland, Washington

High-Resolution Nuclear Magnetic Resonance Investigation of Nanomaterials
L Wang
Pacific Northwest National Laboratory, Richland, Washington

Structural Studies of *Escherichia coli* Formamidopyrimidine DNA N-Glycosylase and Its Main Biological Substrate 8-Oxoguanine
SS Wallace
University of Vermont, Burlington, Vermont
GW Buchko
Pacific Northwest National Laboratory, Richland, Washington

Nuclear Magnetic Resonance Structural Investigations of BRCA1
RE Klevit, PS Brzovic, ME Daley
University of Washington, Seattle, Washington

Structural Proteomics of *Myobacterium tuberculosis*
GW Buchko, MA Kennedy
Pacific Northwest National Laboratory, Richland, Washington
TC Terwilliger
Los Alamos National Laboratory, Los Alamos, New Mexico

Molecular Probes of Quinol Oxidation by the Cytochrome b6f Complex
DM Kramer, IP Forquer, JL Cape
Washington State University, Pullman, Washington
AG Roberts
University of Washington, Seattle, Washington

Electron-Nuclear Double Resonance Analysis of Trityl Radicals
C Mailer
University of Chicago, Chicago, Illinois

Atomic-Level Structure of Silicon and Aluminum in Natural and Synthetic Minerals
NW Hinman
University of Montana, Missoula, Montana

Ultra-High Field Nuclear Magnetic Resonance Studies of Stable Isotope Applications

LA Silks
Los Alamos National Laboratory, Los Alamos, New Mexico

Spatial Properties of Clustered Free Radicals Produced in DNA and Bio-Dosimeters by Ionizing Radiation

JD Zimbrick
Purdue University, West Lafayette, Indiana

Solid-State Zinc-67 Nuclear Magnetic Resonance Studies of Synthetic Metalloprotein Models

G Parkin
Columbia University, New York, New York
AS Lipton, PD Ellis
Pacific Northwest National Laboratory, Richland, Washington

Structural Determination of a Complex Membrane Protein, Diacylglycerol Kinase

CR Sanders
Vanderbilt University, Nashville, Tennessee
FD Soennichsen
Case Western Reserve University, Cleveland, Ohio

Characterization of the Mineral Phases of Matrix Vesicles During Induction of Crystalline Mineral Formation

RE Wuthier
University of South Carolina School of Medicine, Columbia, South Carolina

Nuclear Magnetic Resonance Studies of the Initial Reaction Products of Diacetylbenzene Isomers with Lysine and Proteins

PS Spencer, MI Sabri
Oregon Health Sciences University/Oregon Graduate Institute, Portland, Oregon

Free Radical Processes in Gamma- and Heavy-Ion-Irradiated DNA

D Becker, MD Sevilla
Oakland University, Rochester, Michigan

Pulsed Electric Parametric Resonance Studies of Transition Metal-Exchanged Zeolites and Molecular Sieves

SC Larsen, JF Woodworth
University of Iowa, Iowa City, Iowa

Structure of Telomerase RNA and Telomeric Proteins

G Varani, TC Leeper, SL Reichow
University of Washington, Seattle, Washington

Solid-State Nuclear Magnetic Resonance Characterization of Metal Phosphines
JV Hanna
Australian Nuclear Science and Technology Organization, Menai, New South Wales, Australia

Probing the Mechanism of the Alkaline Phosphatase Reaction by Zinc-67 and Magnesium-25 Nuclear Magnetic Resonance
ER Kantrowitz
Boston College, Chestnut Hill, Massachusetts
AS Lipton, PD Ellis
Pacific Northwest National Laboratory, Richland, Washington

Structure of a Helical Signaling Domain from Cas
KR Ely, K Briknarova
The Burnham Institute, La Jolla, California

Solid-State Nuclear Magnetic Resonance Investigation of Coating Materials Prepared Using the Single-Nucleotide Amplified Polymorphisms Methodology
RA Mantz
Air Force Research Laboratory, Wright-Patterson Air Force Base, Ohio

Solid-State Nuclear Magnetic Resonance Spectroscopy of Half-Integer Spin Quadrupolar Nuclei at High Magnetic Field Strengths: A Continuing Study of Hydrochloride Salts and Zirconium Phosphates
KW Feindel, RE Wasylishen
University of Alberta, Edmonton, Alberta, Canada

An Extended Study of Solid Prototypal Chromium and Molybdenum Compounds Using Chromium-53 and Molybdenum-95 Nuclear Magnetic Resonance Spectroscopy
MA Forgeron, KJ Ooms, RE Wasylishen
University of Alberta, Edmonton, Alberta, Canada

Electron Parametric Resonance and Electron-Nuclear Double Resonance Characterization of Iron and Manganese Containing Spin Systems of Relevance to Proteins, Magnetic Materials, and Oxidation Catalysts
SW Gordon-Wylie
University of Vermont, Burlington, Vermont

Distance Measurements in RNA Using Double Electron-Electron Resonance Spectroscopy with Site-Directed Spin Labeling
N Kim, VJ DeRose
Texas A&M University, College Station, Texas

Nuclear Magnetic Resonance Investigation of Folding and Dynamics of the IkB/NFkB System

G Melacini
McMaster University, Hamilton, Ontario, Canada
EA Komives
University of California, San Diego, La Jolla, California

Biofilm Studies Using Multi-Modal Molecular Imaging Agents

DJ Bornhop
Texas Technical University, Lubbock, Texas
FJ Brockman
Pacific Northwest National Laboratory, Richland, Washington

Protonation State of Nicotine in Tobacco Smoke Particulate Matter by Solid-State Nuclear Magnetic Resonance

DH Peyton
Portland State University, Portland, Oregon
KC Barsanti
Oregon Health Sciences University/Oregon Graduate Institute, Beaverton, Oregon

Germanium Crystal Orientation to Facilitate a Search for Dark Matter Via the Majorana Neutrinoless Double-Beta Decay Experiment

KM Kazkaz, JF Wilkerson
University of Washington, Seattle, Washington

Probing Nanostructural Materials

L Wang
Pacific Northwest National Laboratory, Richland, Washington

Investigating Molecular Recognition and Biological Function at Interfaces Using Antimicrobial and Biomineralization Peptides

ML Cotten, MN Manion, KC Daugherty
Pacific Lutheran University, Tacoma, Washington

Development of Resolution Enhancement Techniques for the Complete Structure Determination of Fully Carbon-13/Nitrogen-15–Labeled Peptides and Proteins Using Solid-State Nuclear Magnetic Resonance

SK Straus, EA Tiong
University of British Columbia, Vancouver, British Columbia, Canada

Continuing Exploration of Nuclear Magnetic Resonance Imaging of Microorganisms in Porous Media

BD Wood
Oregon State University, Corvallis, Oregon
HE Trease
Pacific Northwest National Laboratory, Richland, Washington

High-Field 1Q Magic Angle Spinning and Multi-Quantum Magic-Angle Spinning Solid-State Nuclear Magnetic Resonance Studies of the Dissolution of Montmorillonite Clays Under Alkaline Conditions

GS Crosson, KT Mueller
Pennsylvania State University, University Park, Pennsylvania

Atomic-Level Investigations of Thermal Spring Deposits: Surface Nuclear Magnetic Resonance of Natural Siliceous Sinters

NW Hinman
University of Montana, Missoula, Montana

Structure and Dynamics of MUC1 Immune Recognition: Significance for Breast Cancer Vaccine Design

AP Campbell, MD Diaz, JS Grinstead
University of Washington, Seattle, Washington

MUC1 Humoral Immune Recognition: Mapping Antibody-Tumor Associated Antigen Interactions

AP Campbell, JS Grinstead
University of Washington, Seattle, Washington

Nuclear Magnetic Resonance Characterization of Spider Silk Proteins and the Effect of Processing on Spider Silk Films

RA Mantz, RA Vaia, MO Stone
Air Force Research Laboratory, Wright-Patterson Air Force Base, Ohio

Structural Characterization of Free and Fibronectin-Bound Anastellin

KR Ely, K Briknarova
The Burnham Institute, La Jolla, California

Structural Biology of DNA Repair Proteins: The Nudix Protein Family from the Extremely Radiation-Resistant Bacterium *Deinococcus radiodurans*

GW Buchko, MA Kennedy
Pacific Northwest National Laboratory, Richland, Washington
SR Holbrook
Lawrence Berkeley National Laboratory, University of California, Berkeley, Berkeley, California

Structural Proteomics: Annotating the Genome Using Three-Dimensional Structure

CH Arrowsmith, A Yee
University of Toronto (Univ. Health Network), Toronto, Ontario, Canada
TA Ramelot, MA Kennedy
Pacific Northwest National Laboratory, Richland, Washington

Imaging Beta Amyloid Plaques in a Transgenic Mouse Model of Alzheimer's Disease

JF Quinn
Oregon Health Sciences University/Oregon Graduate Institute, Portland, Oregon

Structural Biology of Mammalian Chromatin High Mobility Group Protein HMGA1 and Ultraviolet-Damaged DNA

MJ Smerdon
Washington State University, Pullman, Washington
GW Buchko, MA Kennedy
Pacific Northwest National Laboratory, Richland, Washington

Crystal Orientation Determination of a Piezoelectric Crystal

MB Toloczko
Pacific Northwest National Laboratory, Richland, Washington

Structural Genomics of Eukaryotic Model Organisms

JM Aramini, GT Montelione
Rutgers University, Piscataway, New Jersey

Variable-Temperature Magic Angle Spinning Nuclear Magnetic Resonance Spectroscopic Study of Incorporated and Sorbed Cesium-133 and Sodium-23 in Zeolitic Minerals

Y Deng, M Flury
Washington State University, Pullman, Washington

Separation of Titanium-47 and Titanium-49 Solid-State Nuclear Magnetic Resonance Lineshapes from Crystalline and Glassy Materials by Static Quadrupolar Carr-Purcell-Meiboom-Gill Experiments

I Farnan
University of Cambridge, Cambridge, United Kingdom
FH Larsen
University of Copenhagen, Copenhagen, Denmark

Defect Dynamics on Crystalline Quartz

JJ Weil, SM Botis, SM Nokhrin
University of Saskatchewan, Saskatoon, Saskatchewan, Canada

High-Field, Solid-State Ruthenium-99 Nuclear Magnetic Resonance Spectroscopy in Inorganic and Organometallic Ruthenium Compounds

RE Wasylishen, KJ Ooms
University of Alberta, Edmonton, Alberta, Canada

Extended Study of Solid Molybdenum and Organometallic Magnesium Compounds Using Molybdenum-95 and Magnesium-25 Nuclear Magnetic Resonance Spectroscopy
RE Wasylishen, MA Forgeron, KJ Ooms
University of Alberta, Edmonton, Alberta, Canada

Electron Paramagnetic Resonance of Non-Heme Iron Proteins
PS Covello, M Loewen
National Research Council/Plant Biotechnology Institute, Saskatoon, Saskatchewan, Canada

Metabonomics Assessment Following ANIT or Acetaminophen Administration to Male Fischer 344 Rats
AF Fuciarelli
Colorado State University, Fort Collins, Colorado

Nuclear Magnetic Resonance Analysis of Small Organics
TC Squier, MU Mayer-Cumblidge
Pacific Northwest National Laboratory, Richland, Washington

Microscopic Characterization of Porosity, Diffusivity, and Tortuosity in Single Particles of Hanford Sediments Using Nuclear Magnetic Resonance Techniques
C Liu
Pacific Northwest National Laboratory, Richland, Washington

Quantifying the Intracellular Spatial State and Dynamics of Water Macromolecule Interactions: Studies of Living Cells
B Franza, RK Kong
University of Washington, Seattle, Washington

Using Nuclear Magnetic Resonance to Identify Potential Geometric Isomers of Metal Chelate Systems
DB Rodovsky, LS Sapochak
Pacific Northwest National Laboratory, Richland, Washington

Interaction of Solution-State Silicates with Trivalent Cations
HM Cho, AR Felmy, OS Qafoku, Y Xia
Pacific Northwest National Laboratory, Richland, Washington

Special Purpose Reconfigurable ASIC Hardware for Accelerating Protein Structure Analysis Software
TJ Conroy
University of Regina, Regina, Saskatchewan, Canada

Investigating the Heterogeneity of Polymer Aging
BR Cherry, TM Alam
Sandia National Laboratory, Albuquerque, New Mexico

Structural Studies of the Hyaluronan Receptor CD-44 and CD44-HA Complex
R Michalczyk, NH Pawley
Los Alamos National Laboratory, Los Alamos, New Mexico

Routine Proton and Carbon-13 Nuclear Magnetic Resonance Analyses of Functionalized Semiconductor Quantum Dots for Biodetection Studies
MG Warner
Pacific Northwest National Laboratory, Richland, Washington

Structure and Dynamics of the 15.5 kD Protein and the 15.5-U4snRNA Complex
PF Flynn, SE Soss
University of Utah, Salt Lake City, Utah

Nuclear Magnetic Resonance Studies of Silica-Polyamine Composites
E Rosenberg, DJ Nielsen
University of Montana, Missoula, Montana

High-Field Aluminum-27 Solid-State Nuclear Magnetic Resonance Studies of Catalytic Zeolites and Weathered Clay Materials
KT Mueller, GM Bowers, GS Crosson
Pennsylvania State University, University Park, Pennsylvania

Structure of the PR Domain of RIZ1 Tumor Suppressor
KR Ely, K Briknarova
The Burnham Institute, La Jolla, California

Solid-State Nuclear Magnetic Resonance Studies on Structures and Oxidation Behavior of Amorphous SiAlCN Ceramics
L An
University of Central Florida, Orlando, Florida

Composite Gadolinium Oxide and Yttrium Phosphate Nanoparticles for Managing Cancer Therapy with Magnetic Resonance Imaging
M Zhang, NJ Kohler, CG Sun
University of Washington, Seattle, Washington

Interaction of *Escherichia coli* Formamidopyrimidine-DNA Glycosylase (FPG) with Damaged DNA Containing an 7,8-Dihydro-8-Oxoguanine Lesion
SS Wallace
University of Vermont, Burlington, Vermont
GW Buchko, MA Kennedy
Pacific Northwest National Laboratory, Richland, Washington

TRAPDOR Experiments on Siliceous Sinters from Thermal Springs
NW Hinman, JM Kotler, LA Strumness
University of Montana, Missoula, Montana

Magnetic Resonance Microscopy of Water Dynamics at Hydrophilic Surfaces
GH Pollack
University of Washington, Seattle, Washington

Complexation of Th(IV) by Organic Acids in Aqueous Solution
HM Cho, AR Felmy
Pacific Northwest National Laboratory, Richland, Washington

Kinetics of Polyphosphate Decomposition in Heterogeneous Environments
BK McNamara, DM Wellman
Pacific Northwest National Laboratory, Richland, Washington

Nuclear Magnetic Resonance Detection of Radiation Damage in Ceramics
I Farnan
University of Cambridge, Cambridge, United Kingdom

Nuclear Magnetic Resonance Analysis of Synthesized Organic Compounds for Modification of Nanostructures
LS Fifield, F Zheng, CL Aardahl, RJ Wiacek
Pacific Northwest National Laboratory, Richland, Washington

Pulsed-Electron Parametric Resonance Studies to Investigate a New Family of Free Radical Spin Traps
GM Rosen
University of Maryland, Baltimore, Maryland

Study of the Structures of Thermally Formed Oxides on Amorphous SiAlCN Ceramics
L An, Y Wang
University of Central Florida, Orlando, Florida
C Wang
Pacific Northwest National Laboratory, Richland, Washington

Development of Multipurpose Tags and Affinity Reagents for Rapid Isolation and Visualization of Protein Complexes
H Cao, TC Squier, DF Lowry, MU Mayer-Cumblidge, P Yan
Pacific Northwest National Laboratory, Richland, Washington

Characterization of Colloid Mobility Using Nuclear Magnetic Resonance Techniques
M Flury, Y Deng
Washington State University, Pullman, Washington

Stablilization of Soil Organic Matter: Land Use, Erosion, and Burial
E Marin-Spiotta, AA Berhe
University of California, Berkeley, Berkeley, California
MS Torn
Lawrence Berkeley National Laboratory, Berkeley, California

High-Field Nuclear Magnetic Resonance Investigations of Strontium-87 in Environmental Samples
GM Bowers, KT Mueller
Pennsylvania State University, University Park, Pennsylvania

Characterization of Folding and Self-Association of the Survival Motor Neuron Protein
RA Nieman
Arizona State University, Tempe, Arizona

Lanthanum-139 Nuclear Magnetic Resonance Studies of Solid Oxo-Coordinate Compounds
RE Wasylishen, KW Feindel, KJ Ooms, MJ Willans
University of Alberta, Edmonton, Alberta, Canada

Investigation of Lineshapes in Fully Carbon-13/Nitrogen-15–Labeled S1 Domain from RNaseE Using Solid-State Nuclear Magnetic Resonance
SK Straus, EA Tiong, PC Dave
University of British Columbia, Vancouver, British Columbia, Canada

Relaxation Nuclear Magnetic Resonance Imaging Investigation of Initiated Polymer Degradation
BR Cherry, TM Alam, MC Celina
Sandia National Laboratory, Albuquerque, New Mexico

Structure Determination of Membrane Proteins from *Mycobacterium tuberculosis*
FD Soennichsen, K Choowongkomon, JL Mills
Case Western Reserve University, Cleveland, Ohio

Structural Genomics of Model Eukaryotic Organisms
JM Aramini, GT Montelione
Rutgers University, Piscataway, New Jersey

Structure and Dynamics of aB57
P Rajagopal, RE Klevit
University of Washington, Seattle, Washington

Solid-State Nuclear Magnetic Resonance Investigation of the Structure of Statherin Protein on the Surface of Hydroxyapatite
GP Drobny, G Goobes
University of Washington, Seattle, Washington

Investigating Molecular Recognition and Biological Function at Interfaces Using Antimicrobial Peptides
ML Cotten, LM Homem, MJ Ellard-Ivey, SM Jones, Y Nikolayeva, TJ Wagner
Pacific Lutheran University, Tacoma, Washington

Solid-State Tungsten-183 Magic Angle Spinning Nuclear Magnetic Resonance at High and Ultra-High Magnetic Fields

JZ Hu, Y Wang, CHF Peden
Pacific Northwest National Laboratory, Richland, Washington
JA Sears
W.R. Wiley Environmental Molecular Sciences Laboratory, Richland, Washington

Structural Studies of Nudix Hydrolyases from *Bacillus anthracis*: The Bacteria That Produces the Deadly Toxin Anthrax

MA Kennedy, GW Buchko
Pacific Northwest National Laboratory, Richland, Washington
SR Holbrook
Lawrence Berkeley National Laboratory, University of California, Berkeley, Berekeley, California

Structural Biology of the Human High Mobility Group A Proteins: Characterizing the Hub of Nuclear Function

RC Reeves, K McAteer
Washington State University, Richland, Washington
GW Buchko, MA Kennedy
Pacific Northwest National Laboratory, Richland, Washington

Study of the Binding of SN-15 to Hydroxyapatite Using $^{15}N\{^{31}P\}$ REDOR

V Raghunathan, JM Gibson, JM Popham, PS Stayton
University of Washington, Seattle, Washington

Drug Interactions of Human and Bacterial Cytochrome P450s Probed by Pulsed Electron Paramagnetic Spectroscopy

AP Campbell, AE Rettie, WM Atkins, AG Roberts, RD Nielsen
University of Washington, Seattle, Washington

Magnetic Resonance Imaging of Gadolinium Phosphate Nanoparticles

A Gutowska
Pacific Northwest National Laboratory, Richland, Washington

Investigation of Soot Morphology and Microstructure with Respect to Oxidation

D Kim
Pacific Northwest National Laboratory, Richland, Washington
A Yezerets
Cummins, Inc., Columbus, Indiana

Probe Performance Testing at 900 MHz

CV Grant, CH Wu, SJ Opella
University of California, San Diego, La Jolla, California
DM Rice
Varian Inc., Palo Alto, California

Development of Organophosphorus Compounds for Solid-State Lighting Applications

AB Padmaperuma, LS Sapochak
Pacific Northwest National Laboratory, Richland, Washington

Nuclear Magnetic Resonance for Catalyst Studies

E Iglesia
University of California, Berkeley, Berkeley, California
CHF Peden, JZ Hu, Y Wang, J Kwak, JE Herrera, J Szanyi
Pacific Northwest National Laboratory, Richland, Washington
J Liu
Sandia National Laboratory, Albuquerque, New Mexico
DA Dixon
University of Alabama, Tuscaloosa, Tuscaloosa, Alabama

Membrane-Organized Chemical Photo-Redox Systems

JK Hurst
Washington State University, Pullman, Washington

Solid-State, Carbon-13 Nuclear Magnetic Resonance Study of Copper Complexation with Standard Ligands

CK Larive
University of Kansas, Lawrence, Kansas
WH Otto
University of Maine, Machias, Machias, Maine

Structure and Dynamics of the Interaction of Membranes with Amyloid Oligomers

JS Barton, CG Glabe
University of California, Irvine, Irvine, California

Staff

David W. Hoyt, Senior Research Scientist**,** Technical Lead
(509) 373-9825, david.w.hoyt@pnl.gov

Araceli Perez, Administrator
(509) 376-2548, araceli.perez@pnl.gov

Sarah D. Burton, Senior Research Scientist
(509) 376-1264, sarah.burton@pnl.gov

Joseph J. Ford, Senior Research Scientist
(509) 376-2446, joseph.ford@pnl.gov

Michael J. Froehlke, Technician
(509) 376-2391, michael.froehlke@pnl.gov

Nancy G. Isern, Research Scientist
(509) 376-1616, nancy.isern@pnl.gov

Donald N. Rommereim, Senior Research Scientist
(509) 376-2671, don.rommereim@pnl.gov

Jesse A. Sears, Jr., Technician
(509) 376-7808, jesse.sears@pnl.gov

We would also like to acknowledge the contributions of Michael K. Bowman, Garry W. Buchko, Herman M. Cho, John R. Cort, Paul D. Ellis, Jian Zhi Hu, Michael A. Kennedy, David W. Koppenaal, Andrew S. Lipton, David F. Lowry, Paul D. Majors, Kevin R. Minard, Theresa A. Ramelot, Robert A. Wind, John R. Bagu, and Kate McAteer.